Renewable and Sustainable Energy Reviews 68 (2017) 1–18

Contents lists available at ScienceDirect

Renewable and Sustainable Energy Reviews

journal homepage: www.elsevier.com/locate/rser

General review and classification of different MPPT Techniques

Nabil Karami[a,*], Nazih Moubayed[b], Rachid Outbib[c]

[a] Department of Mechanical Engineering, Faculty of Engineering 1, Lebanese University, Tripoli, Lebanon
[b] LARGES, CRSI, Faculty of Engineering, Lebanese University, Tripoli, Lebanon
[c] Laboratory of Sciences in Information and Systems (LSIS) Aix-Marseille University, 13013 Marseille, France

ARTICLE INFO

Keywords:
MPP
MPPT
PV
Converter
Power electronics

ABSTRACT

In this paper, the concept of power tracking for PV systems is highlighted and an overview on 40 old and recent Maximum Power Point Tracking (MPPT) methods, available in the literature, is presented and classified. These methods are mathematically modeled and presented in such a way the reader can select the most appropriate method for his own application. A comparative table is presented at the end of the paper to simplify the classification of the different methods.

1. Introduction

A few years ago, researchers started to develop strategies to extract as much power as possible from renewable energy sources and especially from the PV panels. They are used for stand-alone and grid-connected system. First, mechanical systems were developed that move the PV panels so that they receive the maximum solar radiations. Another type of tracker, called electrical Maximum Power Point Tracker (MPPT), is based on moving the operating PV voltage, or current, in order to get the maximum power. This tracker usually requires a switching converter to sweep the PV power. To date, a big number of MPPT algorithms and designs are available in the literature. Each method has its own specifications, limitations and applications. It is convenient to mention that MPPT is not only applied to extract power from PV panels, but also used for different types of renewable energy sources such as fuel cells [1,2], thermoelectric devices [3], etc. In this paper, the MPPT is developed mathematically and a list of 40 different tracking methods, dedicated for PV systems, are discussed.

In general, PV systems are divided into three categories: the stand-alone systems [4,5], the grid-connected systems [6] and the hybrid systems in which PV systems are merged into other types of energy source systems [7,8].

The performance of a PV system depends on the operating conditions. Then, the maximum power extracted from the PV generator depends strongly on three factors: irradiance, cell temperature (ambient temperature), and load profile (load impedance). The output $I - V$ characteristic of a PV module is a function of irradiation and temperature. The irradiation changes affect the PV output current while the temperature changes affect the PV output voltage.

However, PV systems are designed to operate at their maximum output power levels for any solar irradiation intensity and temperature. The factor that determines the PV output power is the load impedance, which can be a DC load with or without batteries. However, it should be noted that such impedance is not constant. When a PV generator is directly connected to a load, the system will operate at the intersection of the $I - V$ curve with the load line, which can be far from the Maximum Power Point (MPP). The maximum power production is based on the load-line adjustment under unstable climatic conditions.

To overcome the undesired effects on the output PV power and draw its maximum power, it is possible to insert a DC/DC converter between the PV panel and the batteries, which can control the seeking of the MPP, besides including the typical functions assigned to the controllers. These converters are normally named as Maximum Power Point Trackers (MPPTs). The input of the DC/DC converter part is formed by the PV array and the output is formed by the batteries and load. A computing system will modify the duty-cycle and implicitly the input impedance of the converter until the system reaches the MPP. On the other hand, their losses have to be small enough so that the efficiency of the overall system is recovered. This could increase the gap between the PV peak power voltage and the voltage at which they are forced to operate in a system without a peak power tracking system.

There are multiple ways to achieve the PV panel and load impedance matching. The system is composed of a DC/DC or DC/AC converter and an MPP computing system. The converter acts as an impedance matching circuit. The MPPT computing system measures the input and/or output voltage and current as well as the climatological variations then computes the power to control the converter input impedance by changing the duty-cycle of the control signal. The PV

* Corresponding author.
E-mail addresses: nabilkarami@hotmail.com (N. Karami), nmoubayed@ieee.org (N. Moubayed), rachid.outbib@lsis.org (R. Outbib).

http://dx.doi.org/10.1016/j.rser.2016.09.132
Received 15 July 2015; Received in revised form 27 July 2016; Accepted 29 September 2016

system scheme is shown in Fig. 1.

The efficiency of a PV plant is affected by the efficiency of the PV panel, the converter/inverter and the efficiency of the MPPT algorithm. The efficiencies of the PV panel and the converter/inverter are not easily improved as they depend on the available hardware technology, but improving the tracking of the MPP with new control algorithms is easier and leads to an increase in the PV power generation.

To date, several MPPT algorithms have been published [9]. They differ in many aspects such as efficiency, convergence speed, complexity, sensors required, cost, hardware implementation, and as well as various other aspects. However, it is pointless to use a more complex or more expensive method if a simpler and less expensive one leads to similar results. This is why some published techniques are not used.

Measuring the efficiency of MPPT algorithms had not been standardized until the European Standard EN 50530 was published at the end of May 2010 [10]. It specifies how to test the efficiency of MPPT methods both statically and dynamically. In any case, there are no publications comparing the results of the different MPPT algorithms under the proposed standard conditions. One of the most important reasons for this is the lack of comprehensive comparative analysis of these algorithms in terms of efficiency. In literature, most of the comparative studies are realized between the systems that include MPPT and those that do not.

2. MPPT modeling

As mentioned before, the irradiation and the temperature affect the PV output power. These atmospheric conditions are not constant during a single day. This causes the MPP to move depending on the temperature and irradiation conditions. Great power losses occur when the operating point is not close to the MPP. Hence, it is essential to track the MPP in any conditions to ensure that the maximum available power is obtained from the PV panel.

When examining the typical PV power and polarization illustrated in Figs. 2 and 3, the point of the maximum power is observed. This point depends mainly on irradiance and temperature. The location of the MPP is unknown, but can be located, either through search algorithms or by calculation models. The curves expressing the behavior of PV power can be written as:

$$P_{PV}(t) = F(V_{PV}(t), I_{PV}(t), \gamma(t)) \tag{1}$$

where γ denotes all the variables other than the current and the voltage and hence defines the power curve at time t. It depends on the PV parameters and on climatological variables.

An MPP tracking technique consists in adjusting the output voltage of the PV to extract the maximum available power at any change in the input (temperature, irradiance). The MPPT is based on the fact that the derivative of the output power with respect to the output voltage is zero at the MPP, positive on the left of the MPP and negative on the right of the MPP (see Fig. 2).

It is convenient to mention that the curves defined by Eq. (1)verify the following property:

$$\begin{cases} \dfrac{dP_{PV}}{dV_{PV}} = 0 & \text{when} \quad V_{PV} = V_{MPP} \\ \dfrac{dP_{PV}}{dV_{PV}} > 0 & \text{when} \quad V_{PV} < V_{MPP} \\ \dfrac{dP_{PV}}{dV_{PV}} < 0 & \text{when} \quad V_{PV} > V_{MPP} \end{cases} \tag{2}$$

Regarding the properties of the curves defined by Eqs. (1) and (2), the tracker strategy consists in respecting the following rule:

$$\frac{dP_{PV}}{dV_{PV}} \cdot \frac{dV_{PV}}{dt} > 0 \tag{3}$$

Deriving the output power with respect to the output voltage leads to:

$$\frac{dP_{PV}}{dV_{PV}} = \frac{d(V_{PV} I_{PV})}{dV_{PV}} = I_{PV} + V_{PV} \frac{dI_{PV}}{dV_{PV}} \tag{4}$$

At MPP, the derivative of power with respect to voltage is zero, therefore:

$$\frac{dP_{PV}}{dV_{PV}} = 0 \Rightarrow \frac{V_{PV}}{I_{PV}} = -\frac{dV_{PV}}{dI_{PV}} \tag{5}$$

The error between the instantaneous and the derivative values is expressed as:

$$\varepsilon = \frac{V_{PV}}{I_{PV}} + \frac{dV_{PV}}{dI_{PV}} \tag{6}$$

Combining Eqs. (2) and (6), the MPP can be tracked by comparing V_{PV}/I_{PV} to dV_{PV}/dI_{PV} as follows:

$$\varepsilon = 0 \leftrightarrow \frac{V_{PV}}{I_{PV}} = -\frac{dV_{PV}}{dI_{PV}} \quad \text{at the MPP} \varepsilon > 0 \leftrightarrow \frac{V_{PV}}{I_{PV}} > -\frac{dV_{PV}}{dI_{PV}} \quad \text{left to the MPP} \varepsilon < 0 \leftrightarrow \frac{V_{PV}}{I_{PV}} < -\frac{dV_{PV}}{dI_{PV}} \quad \text{right to the MPP} \tag{7}$$

Eq. (7) is illustrated by Fig. 3. MPP exists on the peak of the power graph at $I_{PV} = I_{MPP}$ which corresponds to the intersection of dP_{PV}/dV_{PV} curves with the current axis and the intersection of V_{PV}/I_{PV} with the dV_{PV}/dI_{PV} curve.

The dV_{PV}/dI_{PV} and the V_{PV}/I_{PV} curves intersect at the MPP that refers to V_{MPP} on the voltage axis (see Fig. 4). The optimum current I_{MPP} is located at the intersection of the current curve at V_{MPP}.

3. MPPT selection criteria

Having lot of tracking techniques available for PV system, it is not evident to decide which one is the best. when selecting the MPP techniques, the following criteria have to be considered,

3.1. Implementation

The ease of implementation is an important factor in deciding which MPPT technique to use. Some techniques are easily implemented with no need for on-site adjustment or calibration. Other techniques are more complex and their calibration varies with site location and climatic conditions.

3.2. Sensors

The number of sensors required to implement the MPPTs also affects the decision process. In order to track the maximum power, it is

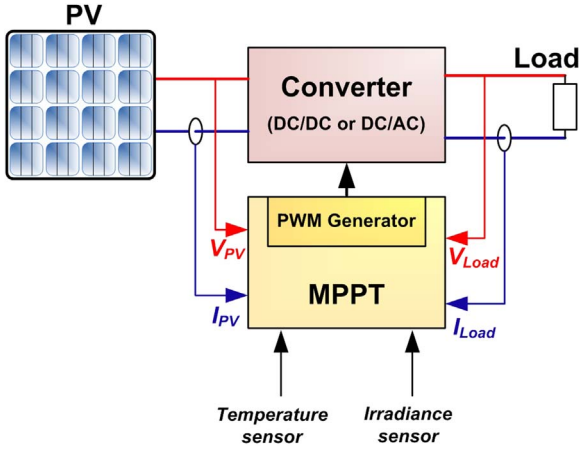

Fig. 1. General scheme of a PV with an MPPT system.

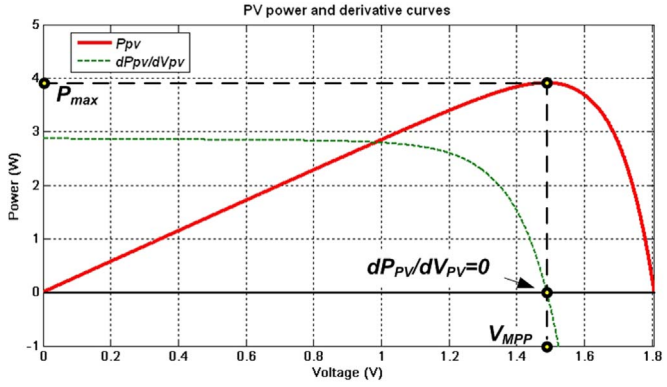

Fig. 2. Power curve and its derivative with respect to V_{PV}.

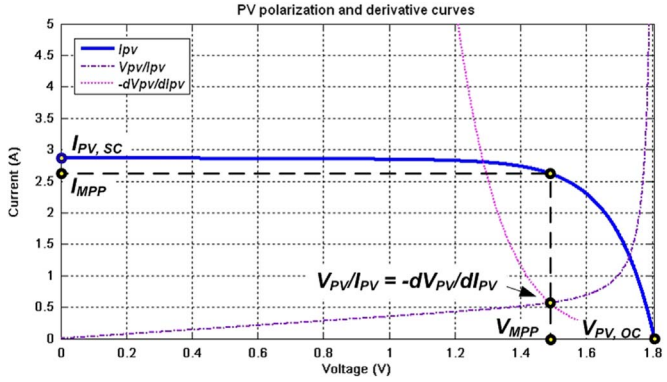

Fig. 3. Intersection of dV_{PV}/dI_{PV} and the V_{PV}/I_{PV} at MPP.

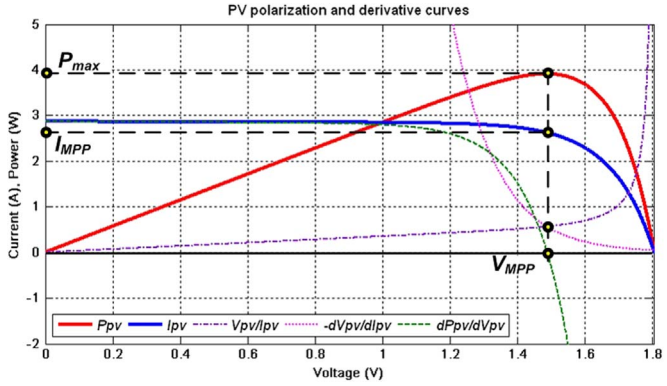

Fig. 4. Polarization curves and derivatives show the location of the MPP, V_{MPP}, and I_{MPP}.

required for the tracker to know the PV inputs (Irradiance and Temperature) and the PV outputs (Voltage and Current). Therefore, four sensors are required. However, some MPPTs use modified techniques to reduce the number of sensors. For example, the Open-Circuit method requires only a voltage sensor to track the maximum power.

3.3. Efficiency

The tracker efficiency is associated to the accuracy of tracking the MPP in minimum time. Some MPPT methods oscillate around the MPP due to its trial techniques in searching the maximum power, which decrease the efficiency of the complete PV system.

3.4. Cost

The cost of a tracking device depends on the system features, its hardware cost, the complexity of the required programming and the number of sensors. Usually, the cost of analog systems is cheaper than the digital ones and the one that are based microprocessor or on PFGA's.

3.5. Application

While studying the methods of tracking techniques, the focus is often put on the tracking control by itself and forget the effect of power maximization on the environmental hardware in which the PV is connected. Usually, a PV system includes batteries in which critical charging and discharging specification have to be considered. Thus, the type of batteries [11–13], the charging techniques and cycles [14–17] should be considered in the selection of the MPPT technique.

4. MPPT method classification

Since the beginning of photovoltaics being used as stand-alone and grid-connected systems, researchers have tried to develop strategies to "squeeze" the PV panel to absorb the maximum power. To date, a big number of MPPT algorithm and designs are available in the literature. Each method has its own specifications, limitations and applications. There is no evaluation study that classifies methods since each one can be suitable for an application and not for another. In this section, tracking methods are categorized by their tracking techniques, which are divided into 5 groups (see Table 1):

- **Tracking techniques with constant parameters:** Methods based on this tracking technique use predefined fixed values that characterize the MPP.
- **Tracking techniques with measurement and comparison:** This technique is based on sensing the external parameters (PV voltage, current, irradiance or temperature) and comparing them with a pre-known MPP.
- **Tracking techniques with trial and error:** These methods use an attempt at calculation and observe the consequent result, which determines the direction criteria for the next attempt in order to reach the MPP.
- **Tracking techniques with mathematical calculation:** These Methods define the location of the MPP based on the mathematical calculation of the available data based on equations.
- **Tracking techniques with intelligent prediction:** These methods use an intelligent learning process that offers the ability to predict the location of the MPP.

5. Tracking techniques with constant parameters

5.1. Method #1: Constant voltage method

The constant voltage (CV) algorithm, also named "*The Best Fixed Voltage (BFV) Algorithm*", is the simplest MPPT control method. The operating point of the PV module is kept near the MPP by regulating the PV voltage and matching it to a fixed reference voltage equal to the V_{MPP} of the characteristic PV module. The CV algorithm (see Fig. 5) omits the effects of irradiance and temperature on the module and assumes that the constant reference voltage is a sufficient approximation of the true MPP. Therefore, the operating point is not exactly matching the MPP and the reference voltage has to be adopted for different geographical positions Fig. 6.

The CV circuit involves only one voltage sensor to measure the PV array voltage V_{PV} to set up the duty-cycle of the DC/DC converter.

It is important to observe that when the PV panel is in low irradiance conditions, the CV technique is more effective than the Perturb and Observe (P & O) method and the incremental conductance (IC) method (analyzed later) [18]. Thanks to this characteristic, the CV method is often combined with other MPPT techniques.

Table 1
List of MPPT methods.

Tracking techniques	#	Tracking methods
Tracking techniques with constant parameters	1	Constant voltage method
	2	Open-circuit voltage method
	3	Short-circuit current method
	4	Open-circuit voltage pilot PV cell method
	5	Temperature Gradient (TG) Algorithm
	6	Temperature Parametric (TP) Method
	7	Feedback voltage or current method
	8	P-N junction drop voltage tracking technique
Tracking techniques with measurement and comparison	9	Look-up table method
	10	Load current or load voltage maximization
	11	Linear current control method
Tracking techniques with trial and error	12	The only-current photovoltaic method
	13	PV Output Senseless (POS) control method
	14	Perturb and Observe (P & O) method
	15	Modified P & O with fixed perturbation step
	16	Conventional P & O with adaptive perturbation
	17	Modified P & O with adaptive perturbation
	18	Three-point weight comparison method
	19	On-Line MPP search algorithm
	20	DC-Link capacitor droop control
	21	Array Reconfiguration Method
	22	MPPT with a variable inductor
Tracking techniques with mathematical calculation	23	State-based MPPT method
	24	Linear reoriented coordinates method
	25	Curve-fitting method
	26	Differentiation method
	27	Slide control method
	28	Current sweep method
	29	dP/dV or dP/dI feedback control
	30	Incremental Conductance method
	31	Variable step incremental conductance method
	32	Variable step-size incremental-resistance method
	33	Parasitic capacitance (*PC*) method
	34	β method
	35	I_{MPP} and V_{MPP} computation method
	36	Methods by modulation
	37	Ripple correlation control
Tracking techniques with intelligent prediction	38	Fuzzy logic control
	39	Neural network
	40	Biological swarm chasing algorithm

5.2. Method #2: Open-circuit voltage method

This method is viable because the PV output voltage at MPP is approximately linearly proportional to its open-circuit voltage, V_{OC}. The relationship is given in Eq. (8) where the proportional constant, k_{OC}, depends mainly on the PV fill factor, the cell technology and on the climatic conditions.

$$V_{MPP} = k_{OC} V_{OC} \quad (k_{OC} < 1) \tag{8}$$

This property can be implemented with the flowchart shown in Fig. 7.a The system is periodically interrupted to measure the open-circuit voltage. Subsequently, the MPP is updated based on the relation given in Eq. (8) and the operating voltage is adjusted to the optimum voltage point. Although, this method is apparently simple, it is difficult to choose an optimal value for the constant k. However, the literature [19–23] reports k_{OC} values ranging from 0.73 to 0.80. The reference voltage represented by the open-circuit voltage, V_{OC}, is chosen as a fixed fraction, and it remains constant for a widely varying climatic

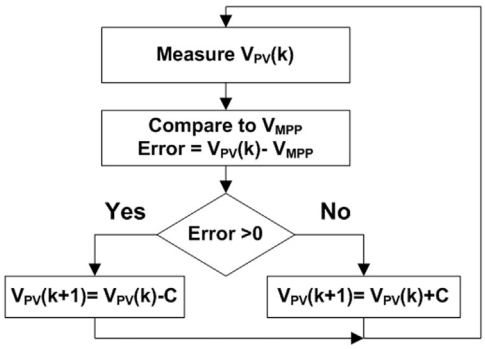

Fig. 5. Constant voltage method flowchart.

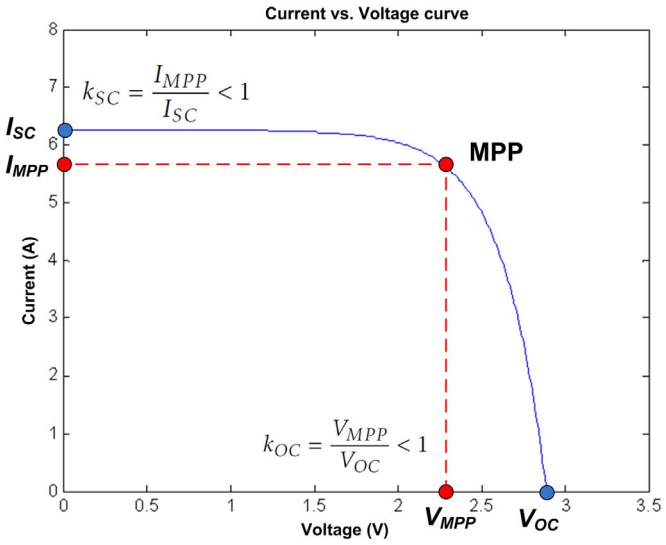

Fig. 6. Relationship between I_{MPP} vs. I_{SC} and V_{MPP} vs. V_{OC}.

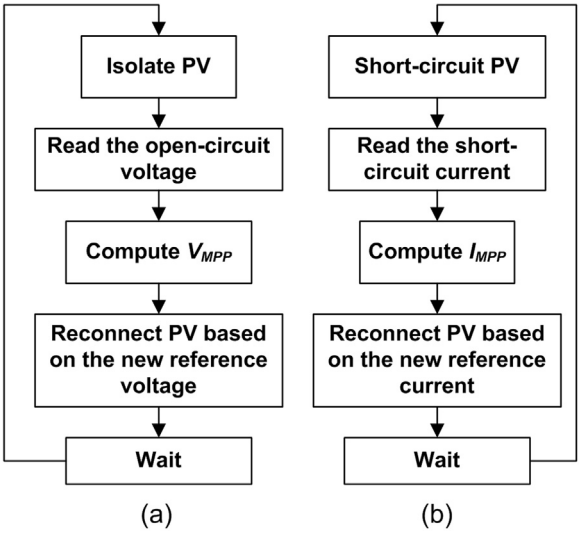

Fig. 7. (a) Open-circuit voltage algorithm, (b) short-circuit current algorithm.

conditions. The accuracy of the operating voltage to match the maximum voltage, V_{MPP}, depends on the choice of this fraction compared with the real relationship of V_{MPP} and V_{OC}. Hence, the extracted power is not maximized.

5.3. Method #3: Short-circuit current method

Similar to the open-circuit tracking method, this tracking method is based on the observed fact of the linear dependency between the PV current at MPP and the short-circuit current, thus satisfying the relationship of Eq. (9). As does the previous method, the proportional constant depends on the PV cell technology, meteorological conditions and the fill factor, mainly. However, the constant k_{SC} can be considered to be around 0.85 for poly-crystalline PV modules [24,25].

$$I_{MPP} = k_{SC} I_{SC} \quad (k_{SC} < 1) \tag{9}$$

However, in many cases, k is determined by performing a PV scanning every several minutes. After k_{SC} is obtained, the system remains with the approximation of Eq. (9), until the next calculation of k_{SC}. The flowchart (see Fig. 7b) of the control is then similar to the open-circuit voltage method. Therefore, this method offers the same advantages and disadvantages as the above-mentioned control method.

5.4. Method #4: Open-circuit voltage pilot PV cell method

This method solves the drawback related to the frequent interruption of the system occurring in two previous methods by using a pilot cell. The PV generator open-circuit voltage is measured from the single cell, which is electrically independent of the rest of the PV module. The resulting values of the ratio, k_{OC}, will be applied to the main PV generator [26–29].

$$V_{MPP} = k_{OC} V_{OC_{pilot}} \quad (k_{OC} < 1) \tag{10}$$

This method uses only one feedback-loop control and avoids the problems caused by the interruptions of the PV operation occurring in the previous methods. On the other hand, this method suffers from the inaccuracy of the cell voltage readings due to partial shading, yield mismatch between the MPP of the pilot cell and the PV generator.

5.5. Method #5: The temperature gradient (TG) algorithm

It can be derived from the PV characteristic equation (i.e Eq. (14)) that the Open-Circuit Voltage (OCV) depends linearly on the cell temperature. Authors in [30] describe the relation as:

$$V_{OC} \cong V_{OC_{STC}} + (T - T_{STC}) \frac{dV_{OC}}{dT} \tag{11}$$

where $V_{OC_{STC}}$ is the open-circuit voltage under Standard Temperature Conditions (STC), T is the actual temperature, T_{STC} is the temperature under *STC* and dV_{OC}/dT is the temperature gradient.

Thus, by measuring the actual temperature, T, the open-circuit voltage, V_{OC} is calculated and the MPP is tracked via the same relation of Eq. (8) given for the *Open-circuit voltage method* in which the panel is disconnected to measure the V_{OC}.

5.6. Method #6: The temperature parametric (TP) method

The same authors [30] of the previous method also model the optimal voltage, V_{MPP}, using experimental tests and formulate it as:

$$V_{MPP} \cong (u + Sv) - T(w + Sy) \tag{12}$$

where u, v, w and y are the PV parameters under different irradiances S. This method requires the measurement of temperature and irradiance to find the optimal voltage.

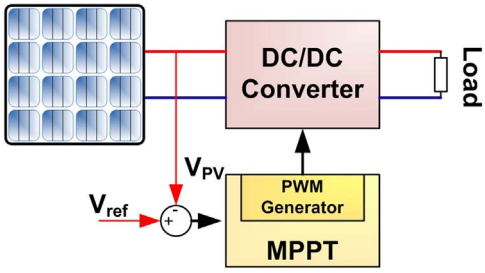

Fig. 8. Voltage-feedback with PWM modulation.

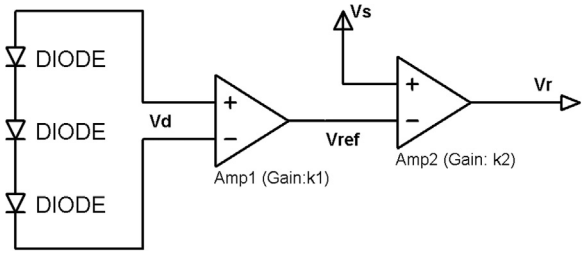

Fig. 9. Control-circuit configuration of the constant voltage tracker.

5.7. Method #7: Feedback voltage or current method

This technique is similar to the Constant Voltage Method. It consists of a simple control system applied to tie the voltage (current) at a constant level [31,32]. Thus, the error between the PV voltage (current) and a constant voltage (current) is used to continuously adjust the duty-cycle (D) of a DC/DC converter to control the PV panel at a predefined operating point, close to the MPP (see Fig. 8). Although this method is economic, simple and uses only one feedback-loop control, but it is not able accommodate to variable climatic conditions.

5.8. Method #8: P-N junction drop voltage tracking technique

This technique is also named "*Excellent Operating Point Tracker*". This is because the temperature characteristic of a PV cell is similar to that of the diode p-n junction. Diodes are installed at the backside of the PV panels so that surface-temperature changes are detected by a voltage drop of the p-n junction, which is used as a reference voltage of the tracker [33]. The reference voltage, V_r, is modeled based on the simplified schematic given in Fig. 9 as follows:

$$V_r = k_2(V_s - V_{ref}) = k_2(V_s - k_1 V_d) \tag{13}$$

where V_s is the output voltage of the PV module, V_{ref} is the reference voltage derived from the amplified value of the forward voltage drop of the p-n junction, V_d. k_1 and k_2 are the gains of the amplifiers Amp1 and Amp2, respectively.

This method considers only the effect of temperature and neglects the effect of irradiance, which leads to a non-accurate tracking technique.

6. Tracking techniques with measurement and comparison

6.1. Method #9: Look-up table method

This technique is based on comparing pre-saved values of all possible climatic conditions with the actual ones. At every cycle, a new operating voltage, V_{MPP}, is determined by the system controller based on the comparison of the measured values of irradiance and temperature with the database saved in the look-up table [34]. The look-up table is generated based on the manufacturer specifications, mathematical modeling of the PV module or via experimental tests on

the PV under different climatic conditions. Therefore, the system requires a large capacity of memory for storing the database of all possible inputs.

6.2. Method #10: Load current or load voltage maximization

When a PV module is connected to a power converter, maximizing the PV power also maximizes the output power of the load. Conversely, maximizing the output power of the converter maximizes the PV power, assuming a lossless converter. It is pointed out that most loads are resistive, voltage-source, current-source, or a combination of these types. For a voltage-source type load, the load current I_{out} should be maximized to reach the maximum output power. For a current-source type load, the load voltage V_{out} should be maximized. For the other load types, either I_{out} or V_{out} can be used. Consequently, only one sensor is needed. Therefore, it is sufficient to maximize either the load current or the load voltage to maximize the power of almost all types of load. In most PV systems, a battery is used as the main load or as a backup, and a positive feedback is used to control the power converter such that the load current is maximized and the PV module operates close to the MPP. Based on this method, another method called "only current PV method" is discussed below. Note that exact operation at the MPP is hardly ever achieved because this MPPT method is based on the assumption that the power converter is lossless [35–39].

6.3. Method #11: Linear current control method

The main idea behind this method is the graphical interpretation of the solution of two algebraic equations as the intersecting point of two curves on the phase plane [40]. This method is easily implemented and its MPP tracking is instantaneous.

First, the simplified $I-V$ characteristic of a PV module is given by:

$$I_{PV} = I_{ph} - I_s \quad (e^{\lambda(V_{PV}+I_{PV}R_s)} - 1) \tag{14}$$

where $\lambda = q/(AkT)$, A is the ideality factor, k the Boltzmann constant and T is the temperature of the cell

Thus, for the proposed MPPT controller, the first curve is represented by $f(P_{PV}, I_{PV}) = 0$ on the $P-I$ curve as follows:

$$f(P_{PV}, I_{PV}) = P_{PV} - V_{PV}I_{PV} = P_{PV} - \frac{1}{\lambda}I_{PV}\ln\left[\frac{I_{ph}+I_s-I_{PV}}{I_s}\right] - I_{PV}^2R_s = 0 \tag{15}$$

Second, at the maximum output power point, the necessary condition is the following:

$$\frac{dP_{PV}}{dI_{PV}} = 0 \tag{16}$$

It follows from Eqs. (14) and (15) the second maximum output power constraint equation is:

$$g(P_{PV}, I_{PV}) = P_{PV} - \frac{1}{\lambda}I_{PV}\ln\frac{I_{PV}^2/\lambda}{(P_{PV}-I_{PV}^2R_s)I_s} - I_{PV}^2R_s = 0 \tag{17}$$

It is interesting to see that for a practical PV module Eq. (17) can be approximated by a linear line to simplify the hardware implementation, as shown in Fig. 10.

7. Tracking techniques with trial and error

7.1. Method #12: The only-current photovoltaic method

This method is based on maximizing the output power by using the PV current only [41]. The system is considered connected to a battery via a DC/DC converter, thus the output voltage which is the battery voltage, V_{bat}, is assumed constant whatever the duty cycle, D, of the PWM control signal (see Fig. 11). In case of a buck converter, the

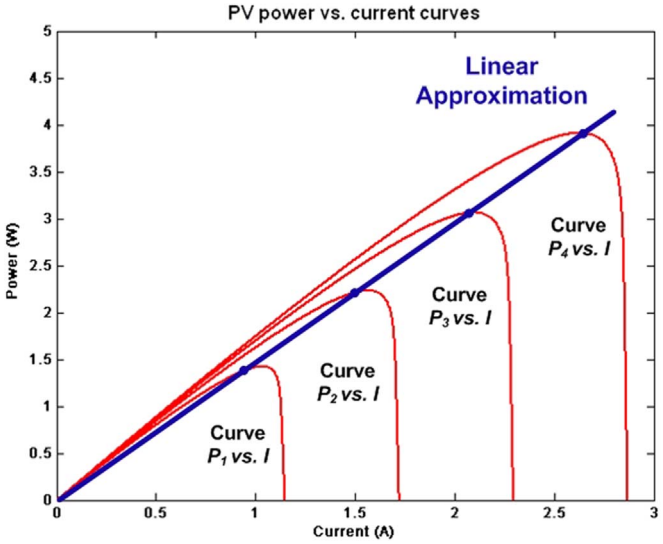

Fig. 10. MPP is located at the intersecting points of the linear approximation curves.

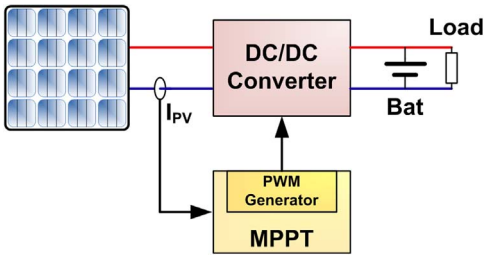

Fig. 11. Block diagram of the only-current method.

battery voltage is given as:

$$V_{bat} = \frac{t_{on}}{T}V_{PV} = DV_{PV} \tag{18}$$

where T is the period and t_{on} is the ON time of the PWM signal.

The converter input power is given as:

$$P_{in} = V_{PV}I_{PV} \tag{19}$$

Replacing Eq. (18) in (19) leads to a new form of power as:

$$P_{in} = V_{bat}\frac{I_{PV}}{D} = V_{bat}P_{Buck}^* \tag{20}$$

where P_{Buck}^* is considered as the ratio of the PV current to the duty cycle:

$$P_{Buck}^* = \frac{I_{PV}}{D} \tag{21}$$

For a constant battery voltage, it can be demonstrated that P_{in} versus D and P_{Buck}^* versus D present the same maximum points for the same duty-cycle values. The algorithm of this method, given in Fig. 12, can be explained as follows: The tracking process starts with an initial duty ratio. First, the PV current $I_{PV}(t)$ is measured and P_{Buck}^* is computed. Then, the duty-cycle is increased by ΔD_1. Second, the PV current $I_{PV}(t+Dt)$ is measured and $P_{Buck}^*(t+Dt)$ is computed again. After collecting the present and the past data of P_{Buck}^*, the controller makes a decision, based on Eqs. (22) and (23), on whether to decrease or increase the duty-cycle ratio depending on the location of the operating point. This tracking process repeats itself indefinitely until the MPP is reached.

$$\Delta P = P_{Buck}^*(t+\Delta t) - P_{Buck}^*(t) \tag{22}$$

and

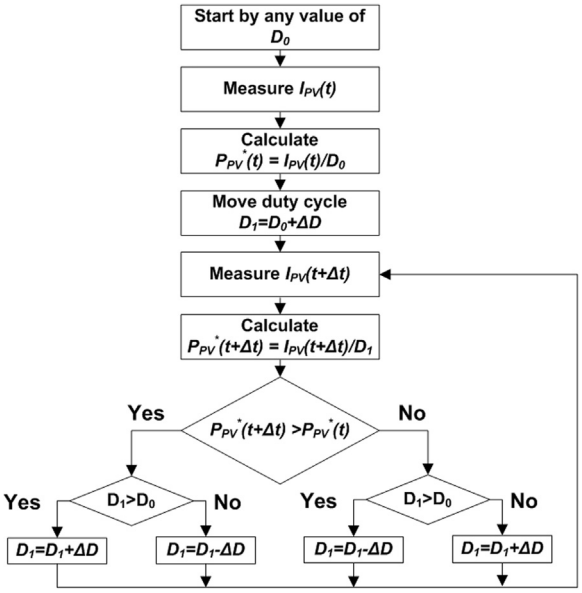

Fig. 12. Flowchart of the only-current photovoltaic method.

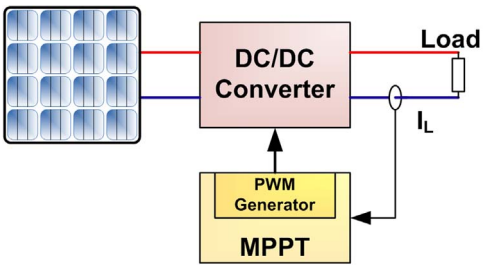

Fig. 13. POS block diagram.

$$\Delta D = D(t + \Delta t) - D(t) \tag{23}$$

This method has a major advantage when compared with other direct methods, which is that it uses the PV current. In addition, this method operates effectively even for fast climatic condition variations [39]. Furthermore, even though this description is made for a buck DC/DC converter, it can be proved that this method is suitable for any DC/DC topology, as reported in [42].

7.2. Method #13: PV output senseless (POS) control method

This technique is dedicated for huge PV generation systems, where the tracker considers only the current flowing to the load (see Fig. 13). In a huge PV power source, the voltage drop across the load is negligible, thus extracting the maximum current is approximately proportional to extracting the maximum power. Therefore, the POS MPPT can be applied to PV generation systems with a simple algorithm, presented in Fig. 14 [43]. The power conversion system is controlled by a PWM signal and the structure of the control circuit is simple. In a large PV generation system, the system can be operated effectively and much more safely, since the voltage and current feedback of PV modules are not needed.

7.3. Method #14: Perturb and observe (P&O) method

The P&O method is one of the most used methods in practice and by the majority of authors [44–48]. This method is based on the trial and error process in finding and tracking the MPP. At every cycle, the tracking controller measures the PV current and voltage and deduces

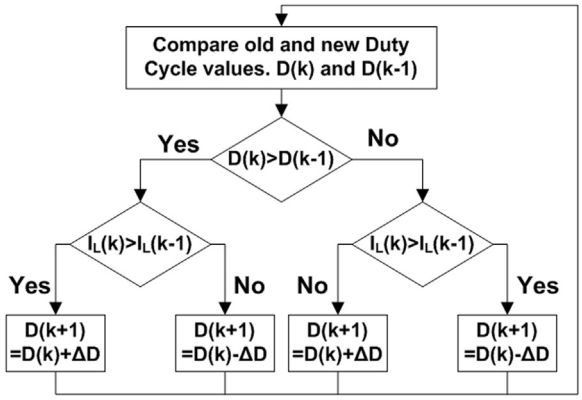

Fig. 14. POS flowchart.

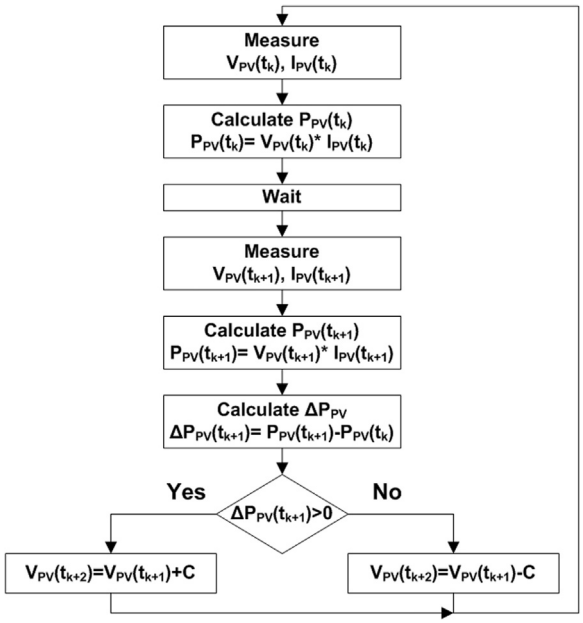

Fig. 15. Conventional P&O algorithm flowchart.

the actual PV power, then perturbs the operating point by sweeping the operating voltage and monitoring the variation of power. If the power increases, the next perturbation of the operating voltage should be in the same direction. However, if the power decreases, the operating voltage is perturbed in the opposite direction. This scenario is repeated until reaching the MPP. The maximum point is reached when $dP_{PV}/dV_{PV} = 0$. The basic flowchart of the P&O algorithm is shown in Fig. 15. The block diagram of conventional P&O is shown in Fig. 16a.

One of the major advantages of this method is that the knowledge of the PV characteristics is not required and is applied to all PV modules. However, this method suffers several drawbacks, as reported in [49,50]. The tracking algorithm depends on two main criteria, the speed of tracking and the step of perturbation. For fixed perturbation values, the steady-state oscillations are proportional to the step value. Large step values cause higher oscillations. Unfortunately, smaller step values result in a slower response. Hence, the famous trade-off problem between faster response and steady-state oscillations is inherent. Moreover, the perturbation step value is not generic; therefore, MPPT using a fixed step is system dependent [51–65]. For enhanced performance, a variable perturbation step is utilized. Initial challenges use variable perturbation values depending on the output power. Although these techniques are not truly adaptive, they present enhanced behavior relative to their fixed perturbation counterparts [66].

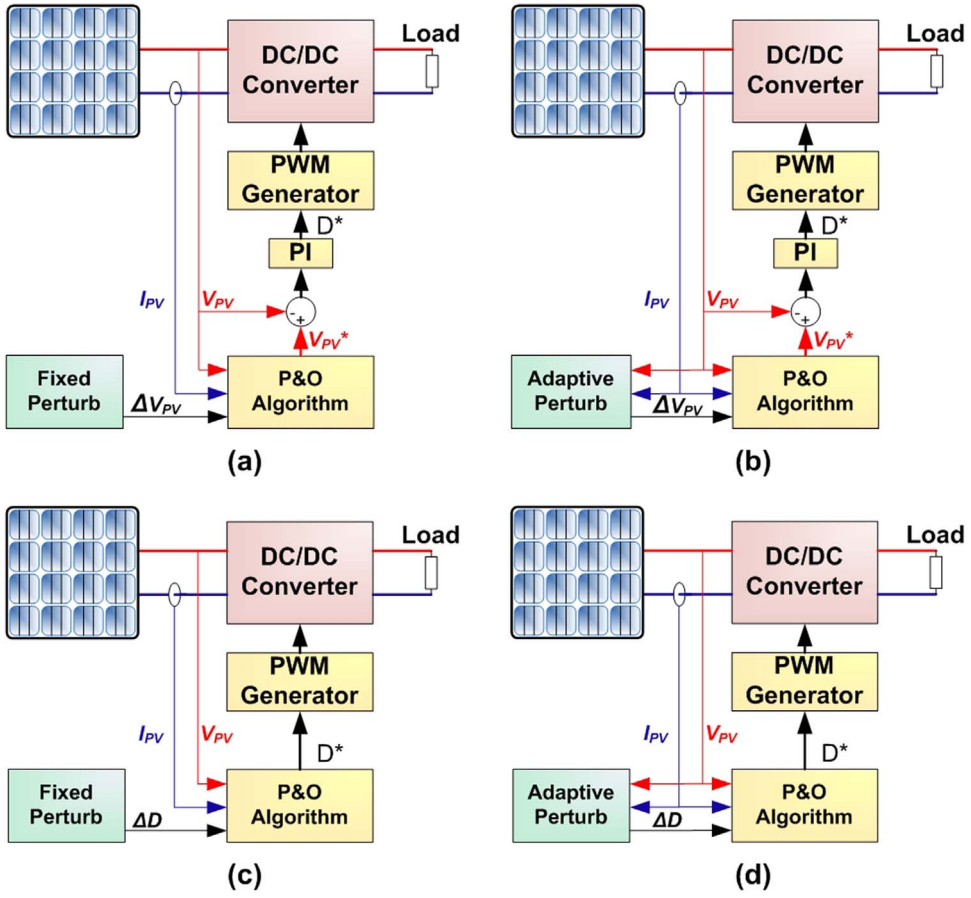

Fig. 16. Various P & O block diagram topologies. (a) Conventional P & O with fixed perturbation step. (b) Conventional P & O with adaptive perturbation step. (c) Modified P & O with fixed perturbation step. (d) Modified P & O with adaptive perturbation step.

Other techniques propose true adaptive modifications, but suffer from a high computational load due to aggressive derivatives [23] and need initial user-dependent constants for the perturbation step adaptation. Therefore, modified techniques of P & O are formulated according to the controlled variable output from MPPT block and the step generation value.

7.4. Method #15: Modified P & O with fixed perturbation step

In this technique, the converter duty ratio is used as the perturbed signal instead of the module voltage. This simplifies the control process as it eliminates the PI/hysteresis controller after the MPPT block, enabling direct control of the converter duty-cycle. The perturbation step is fixed and designer dependent, thus the previously mentioned trade-off problem persists. Fig. 16c shows the Modified P & O with fixed perturbation step block diagram. In order to improve the performance of P & O techniques, the adaptive calculation of the perturbation value is utilized instead of the fixed values used in the classical P & O method.

7.5. Method #16: Conventional P & O with adaptive perturbation

This method, shown in Fig. 16b, consists in varying the perturbation value during the hill-climbing process. Initially, the voltage perturbation step is set to 10% of the open-circuit voltage. Each successive step is 50% of the previous one until the perturbation value is 0.5% of the open-circuit voltage. Despite the acceptable results this method shows, it is still not fully adaptive as the steps are predetermined. Moreover, it depends on the open-circuit voltage, which varies with the environmental conditions [23,66]. Hence, the method is not fully adaptive either.

7.6. Method #17: Modified P & O with adaptive perturbation

Advanced attempts are proposed to improve the P & O in order to find the best value for the perturbation step to reach the fastest tracking time with less oscillation [44,67,68]. The modified P & O using an adaptive perturbation step is defined by formulating the duty cycle step-size as:

$$d(k) = d(k-1) \pm \frac{|\Delta P/\Delta d|}{|P/d|} \tag{24}$$

Despite good performance, this technique suffers several demerits, such as the high computational load versus accuracy trade-off and the predefined constants dependency. Modified P & O with adaptive perturbation step block diagram is shown in Fig. 16d.

7.7. Method #18: Three-point weight comparison method

This method avoids the oscillation problem of the P & O algorithm that compares only two points; the present and the previous points. The algorithm of the three-point weight comparison, illustrated in Fig. 18, runs periodically by perturbing the PV terminal voltage and comparing the PV output power on three points of the PV curve. The three points are defined as follows:

- the current operation point *A*
- a point, *B*, perturbed from point *A*
- a point, *C*, doubly perturbed in the opposite direction from point *B*.

Thus, nine possible cases have to be implemented in the control circuit to reach the MPP. These cases are illustrated in Fig. 17. The

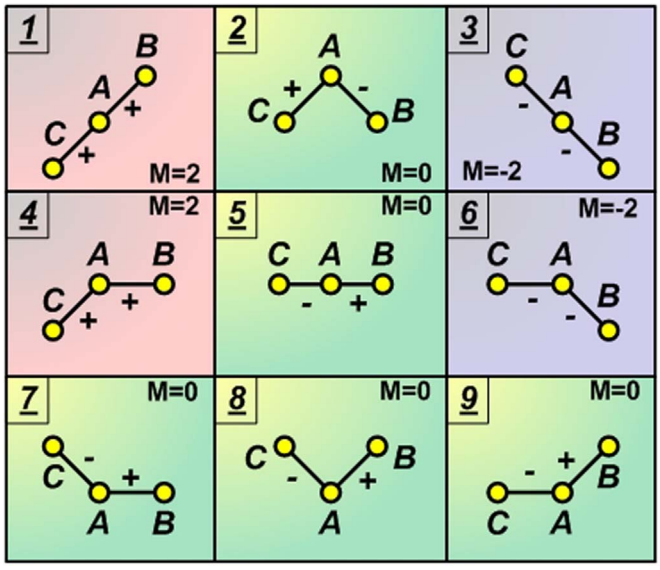

Fig. 17. Nine possible cases of power variation for the three-point weight comparison algorithm.

algorithm is as follows:

- the status is positively weighted if the power at *B* is greater than or equal to the power at point *A*, otherwise, the status is negatively weighted;
- the status is positively weighted when the power at *C* is smaller than the power at point *A*, otherwise, the status is negatively weighted;
- based on the three measured points, if two of them are positively weighted, the duty-cycle of the converter should be increased. Otherwise, if two of them are negatively weighted, the duty-cycle should be decreased. The MPPT is reached when one is positive and the other is negative [60] .

7.8. Method #19: On-line MPP search algorithm

The main task of this algorithm is to determine the reference maximum power value and compare it to the existing power. The difference is called the maximum power error. The PV module operates at the MPP when the difference is zero (see Fig. 19).

Initially, the reference values of MPP power P_{ref} and current I_{ref} are set to zero, and the voltage V_{ref} is set to the open-circuit voltage V_{OC} of the PV module. At each sampling instant, the difference P_{error} between the reference initial value of P_{ref} and the current operating power, P_{actual}, of the PV module is calculated and compared to $P_{tolerance}$. If the difference P_{error} is smaller than the accepted error, $P_{tolerance}$, the currently assigned initial values P_{ref}, V_{ref} and I_{ref} are maintained unchanged and taken as the operating power, voltage and current corresponding to MPP. These values are reassigned by $P_{actual,ref}$, $V_{actual,ref}$, and $I_{actual,ref}$, and are used as reference maximum power quantities for the current sampling. For example, $P_{actual,ref}$ is used as reference maximum power, RMP, for the present sample. When starting for the next sample, these previously obtained MPP quantities, $P_{actual,ref}$, $V_{actual,ref}$, and $I_{actual,ref}$ are taken as the new initial values for P_{ref}, V_{ref}, and I_{ref}. If P_{error} is greater than the $P_{tolerance}$, then the algorithm searches for a new MPP. If the operating power P_{actual} is greater than the current MPP power value, P_{ref}, then the current PV module operating power, P $_{actual}$, voltage, V_{actual}, and current, I_{actual}, are assigned to $P_{actual,ref}$, $V_{actual,ref}$, and $I_{actual,ref}$, respectively.

This search algorithm is based on the operating power of the load. The PV output voltage, V_{actual}, is adjusted by the algorithm to increase or to decrease the operating current of the load to the level of the PV MPP current, $I_{actual,ref}$, which yields the MPP power $P_{actual,ref}$.

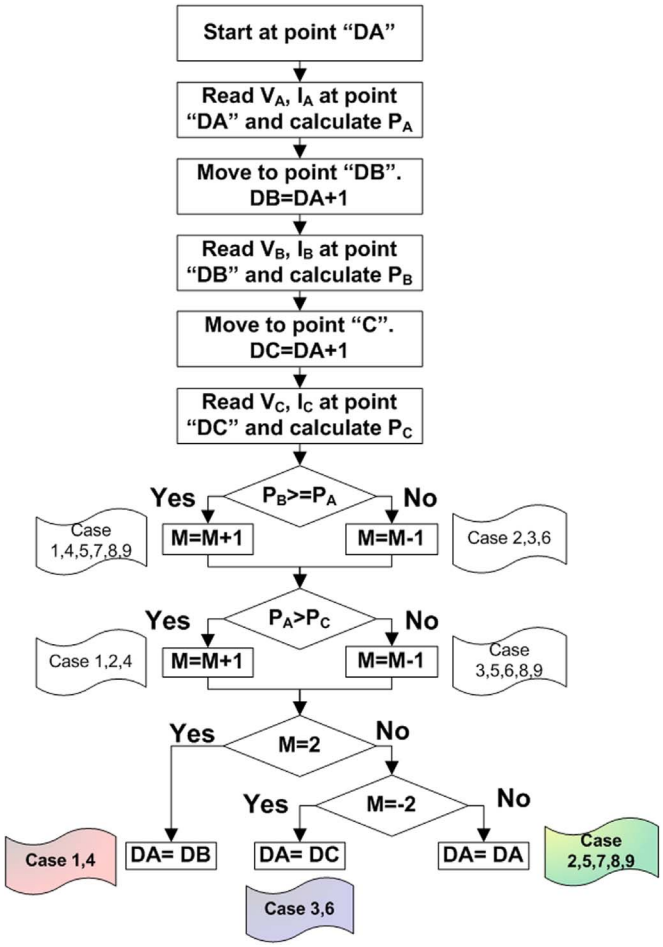

Fig. 18. Three-point weight comparison flowchart.

This algorithm will not be able to determine the MPP if the load power or current is small. In this case, additional loads should be connected to increase the PV module current so that the PV module can be operated at the MPP. If the reference MPP is changed due to a climatic variation, the algorithm adjusts the module voltage and finds the new MPP [69].

7.9. Method #20: DC-Link capacitor droop control

This technique is specifically designed to work with a PV system that is cascaded with an AC inverter as shown in Fig. 20 [70,71]. In case of a boost converter connected between the PV and the AC system, the output voltage, V_{link}, and the input voltage, V_{PV}, are related by the following equation:

$$D = 1 - \frac{V_{PV}}{V_{link}} \tag{25}$$

where *D* is the duty ratio of an ideal boost converter.

The control of the MPPT techniques is based on detecting the voltage drop across the DC-link capacitor V_{link}. By considering it constant, increasing the inverter current increases the power coming out from the boost and consequently increases the power coming out from the PV module. The voltage V_{link} can be kept constant as long as the power required by the inverter does not exceed the maximum power available from the PV module. When exceeding the maximum PV power, the voltage across the capacitor V_{link} starts drooping. Right before that point, the current control command I_{Peak} of the inverter is at its maximum and the PV module operates at the MPP. The AC system line current is fed back to prevent V_{link} from drooping and *D* is

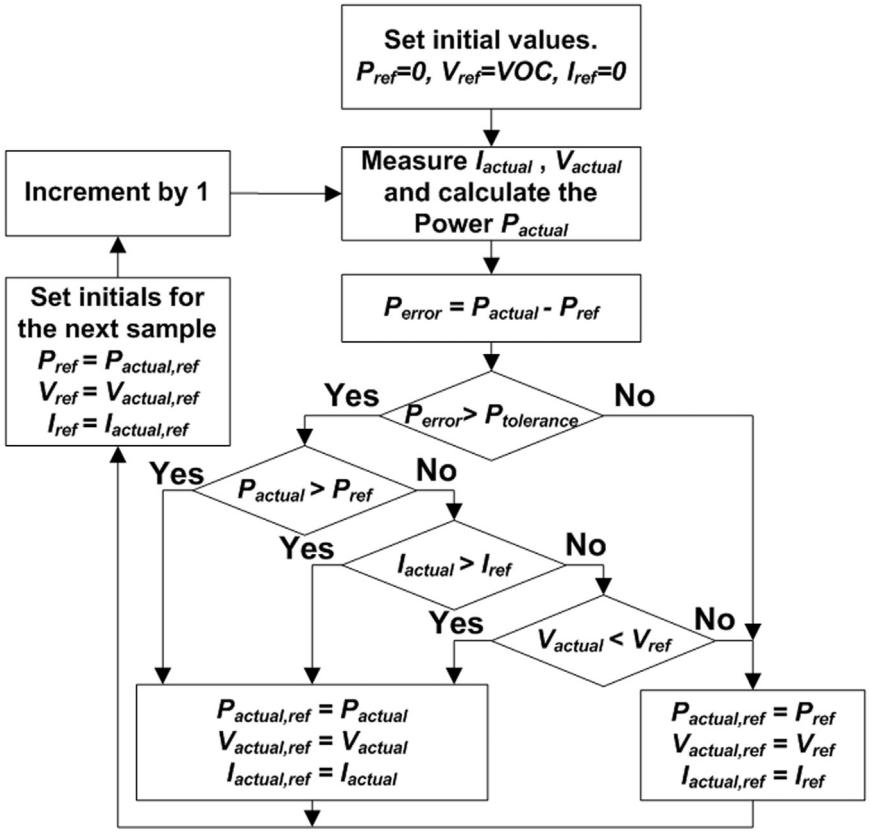

Fig. 19. Flowchart of the on-line search algorithm.

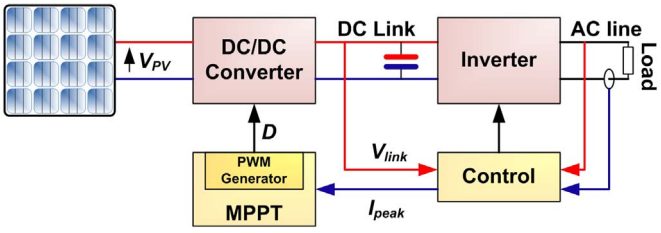

Fig. 20. Topology of a DC-link capacitor droop control.

optimized to bring I_{Peak} to its maximum.

7.10. Method #21: Array reconfiguration method

In this method, the PV arrays are arranged in different series and parallel combinations such that the resulting MPPs meet a specific load requirement. This method is time-consuming and the MPP tracking in real-time is not obvious [72]. The solar array is going to be divided into two modules. The first one represents the basic module, and the second will be divided into sub-modules. There are three ways in which the modules can be arranged: parallel, series, and parallel-series.

7.11. Method #22: MPPT with a variable inductor

This technique considers interfacing a buck converter with the PV and the load. A buck converter is made of a series switching component and an LC filter. In this technique, the inductor is mainly used and a relationship between the minimum inductor value and the PV current is modeled mathematically to achieve the MPPT [73]. The minimum inductance ensuring a Continuous Current Mode (CCM) in a buck circuit is given by:

$$L_{min} = \frac{R_L(1-D)}{2f_s} \tag{26}$$

where R_L is the load resistance, D is the duty cycle of the PWM signal applied to the buck switch, and f_s is the switching frequency.

The input current, I_{PV}, and the output current, I_L, of a buck converter are related as:

$$I_{PV} = I_L D \tag{27}$$

On the other hand, the input impedance R_i of the buck and the output load resistance R_L are related to each other as:

$$R_i = \frac{V_{PV}}{I_{PV}} = \frac{1}{D^2}\frac{V_L}{I_L} = \frac{1}{D^2}R_L \tag{28}$$

where V_L and I_L are the load voltage and current, respectively.

Combining Eqs. (26)–(28) leads to a model relating the minimum inductance to the PV current,

$$L_{min} = \frac{D(1-D)V_{PV}}{2f_s I_L} = \frac{D^2(1-D)V_{PV}}{2f_s I_{PV}} \tag{29}$$

By considering a constant PV voltage over the full range of solar intensities, the minimum inductance becomes a function of the duty cycle D and the output current of the PV panel I_L or a function of the duty cycle D and the load current I_L.

8. Tracking techniques with mathematical calculation

8.1. Method #23: State-based MPPT method

The PV system is represented by a state space model, and a nonlinear time-varying dynamic feedback controller is used to track the MPP. Simulations confirm that this technique is robust and insensitive to changes in system parameters and that MPPT is achieved even with changing atmospheric conditions, and in the presence of

multiple local maxima caused by partially shaded PV array or damaged cells. However, no experimental verification is given [5,74].

8.2. Method #24: Linear reoriented coordinates method (LRCM)

This method iteratively solves the MPP equation of the PV array characteristic, where the equation is manipulated to find an approximate symbolic for the MPP. It requires the measurement of V_{OC} and I_{SC} and other constants representing the PV array characteristic curve. LRCM approximates the MPP to 0.3% based only on simulation results [75]. Using the $I-V$ curve, a linear current equation can be determined from the initial and final values. The slope of the $I-V$ curve at the knee point is approximated by the slope of the linear current equation [5].

8.3. Method #25: Curve-fitting method

The nonlinear characteristic of a PV cell can be modeled using numerical approximations or mathematical equations [76,77]. However, their resolution is impossible by analog control and very difficult by conventional digital control. Hence, their application does not seem suitable for obtaining the MPP. Therefore, [78] proposes fitting the P-V characteristic curve by the Eq. (30) where a, b, c and d are coefficients determined by the sampling of the PV power, current and voltage in the required interval.

$$P_{PV} = aV_{PV}^3 + bV_{PV}^2 + cV_{PV} + d \tag{30}$$

Thus, the voltage at which the maximum power becomes maximized is obtained by:

$$V_{MPP} = \frac{-b\sqrt{b^2 - 3ac}}{3a} \tag{31}$$

The calculation process should be repeated at a fast rate to get the higher tracking accuracy. This method requires the knowledge of the PV physical parameters and the manufacturing specifications, as well as the accurate expressions used for all climatological conditions. For all the above-mentioned reasons, the control system requires a large memory capacity and a heavy processor for the calculation of the mathematical equations.

8.4. Method #26: Differentiation method

This technique is based on the property in which the MPP is located by solving Eq. (32) [53,67].

$$\frac{dP_{PV}}{dt} = V_{PV} \quad and \quad \frac{dI_{PV}}{dt} + I_{PV}\frac{dV_{PV}}{dt} = 0 \tag{32}$$

However, the system hardware requires a powerful processor to quickly solve Eq. (32). Real-time adjustment of the operating point requires at least eight calculations and measurements:

C1: Measure the PV voltage V_{PV},
C2: Measure the PV current I_{PV},
C3: Measure the change in voltage, dV_{PV}, during the perturbation time (dt),
C4: Measure the change in current, dI_{PV}, during the perturbation time (dt),
C5: Calculate the product dV_{PV} with dI_{PV},
C6: Calculate the product I_{PV} with dV_{PV},
C7: Calculate the resulting sum $V_{PV} \times dI_{PV} + I_{PV} \times dV_{PV}$,
C8: Compare the sum to an equal perturbation on the opposite side of the operating point.

Furthermore, if the sum is different from zero, a ninth calculation process should be done on the sign of the dP_{PV} sum, which indicates the adjustment direction of the operating point to reach the MPP.

8.5. Method #27: Slide control method

This technique is based on calculating the variation of the PV power versus the PV voltage as:

$$S = \frac{dP_{PV}}{dV_{PV}} = I_{PV} + V_{PV}\frac{dI_{PV}}{dV_{PV}} \tag{33}$$

where S determines the position of the operating voltage based on the location of the MPP. This tracking technique is achieved by the control of a DC/DC converter. The state, u, of the power switching device (i.e the MOSFET or the IGBT transistor) is used to model this technique, where u=1, means that the power switch is closed, while for u=0, the switch is opened. Thus, the control technique uses u to track the MPP as:

$$u = \begin{cases} 0 & S \geq 0 \\ 1 & S < 0 \end{cases} \tag{34}$$

This technique generally uses a hysteretic mode control of the DC/DC converter. It is very fast, as reported in [79] but suffers from an unstable switching frequency of the switching components.

8.6. Method #28: Current sweep method

The proposed method is based on the determination of the derivative of the panel output power with respect to the panel current while the panel current is manipulated as a decaying exponential sweep function. The current sweep [80] method uses a sweep waveform for the PV current such that its $I-V$ characteristic is obtained and updated at fixed time intervals. The V_{MPP} can then be computed from the characteristic curve at the same intervals. The sweep waveform of the panel current can be manipulated as a predetermined function of time.

$$I_{PV}(t) = f(t) \tag{35}$$

The power of the panel along this sweep waveform will be:

$$P_{PV}(t) = V_{PV}(t)I_{PV}(t) = V_{PV}(t)f(t) \tag{36}$$

At MPP, the derivative of $P_{PV}(t)$ is zero,

$$\frac{dP_{PV}(t)}{dt} = V_{PV}(t)\frac{df(t)}{dt} + f(t)\frac{dV_{PV}(t)}{dt} = 0 \tag{37}$$

Further simplification of Eq. (37) is obtained by selecting the sweep waveform directly proportional to its derivative.

$$f(t) = k\frac{df(t)}{dt} \tag{38}$$

where k is a real constant. By selecting $f(t)$ in this manner, the MPP condition of Eq. (37) simplifies to:

$$\frac{dP_{PV}(t)}{dt} = \frac{df(t)}{dt}\left(k\frac{dV_{PV}(t)}{dt} + V_{PV}(t)\right) = 0 \tag{39}$$

Assuming the derivative of $f(t)$ is non-zero in the range of the sweep waveform, both sides of Eq. (39) can be divided by $df(t)/dt$ with $f(t) = I_{PV}(t)$ to obtain the following relation:

$$\frac{dP_{PV}}{df(t)} = \frac{dP_{PV}}{dI_{PV}} = k\frac{dV_{PV}(t)}{dt} + V_{PV}(t) \tag{40}$$

The maximum power point condition given by Eq. (39) can be tested only using the voltage V_{PV} and its derivative,

$$k\frac{dV_{PV}(t)}{dt} + V_{PV}(t) = 0 \tag{41}$$

The solution of the differential equation (Eq. (38)) is unique and is:

$$f(t) = c.\ e^{t/k} \tag{42}$$

where c is the arbitrary constant of the general solution. Note that in

Eq. (42), if k is selected as a negative real number, the sweep waveform corresponds to an exponentially decreasing function with a time constant $\tau = -k$, and in that case, c corresponds simply to the maximum current I_{max} at the beginning of the sweep when t=0. The selection of the constants $k < 0$ and $c = I_{max}$ simplifies the generation of the sweep waveform since Eq. (42) corresponds to the voltage (or current) of a capacitor discharging through a resistor. At the instant when the test condition is satisfied, the voltage V_{PV} can be held by an analog hold circuit as the set point of the controller of the chopper for the period of power delivery to the load and batteries. This MPPT technique is only feasible if the power consumption of the tracking unit is lower than the increase in power that it can bring to the entire PV system.

8.7. Method #29: dP/dV or dP/dI feedback control

This method consists in computing the slope dP_{PV}/dV_{PV}, or dP_{PV}/dI_{PV}, of the PV power curve and feed the power converter with some control to drive it to zero. Based on the computed sign of the past few cycles, the duty-cycle of the power converter is either incremented or decremented to reach the MPP, thanks to the microcontrollers and the digital signal processors being able to handle complex computations to determine the MPP. [81].

8.8. Method #30: Incremental conductance method

The Incremental Conductance (IC) method consists in differentiating the PV power with respect to voltage. MPP is located when the differentiation result is zero [82]. Therefore, The MPPT controller solves the power using Eqs. (43) and (44).

$$\frac{dP_{PV}}{dV_{PV}} = \frac{d(V_{PV}I_{PV})}{dV_{PV}} = I_{PV} + V_{PV}\frac{dI_{PV}}{dV_{PV}} = 0 \tag{43}$$

hence,

$$\frac{V_{PV}}{I_{PV}} = -\frac{dV_{PV}}{dI_{PV}} \tag{44}$$

Eqs. (43) and (44) are represented graphically in Figs. 3 and 4.

The left-hand side of Eq. (44) represents the instantaneous conductance, whereas the right hand side represents the opposite of its incremental conductance. On the other hand, the incremental variations, dV_{PV} and dI_{PV}, can be approximated by the increments of both parameters ΔV_{PV} and ΔI_{PV} using the measured values of V_{PV} and I_{PV} at different instants. Therefore, parameters can be expressed as:

$$dV_{PV}(t_2) \approx \Delta V_{PV}(t_2) = V_{PV}(t_2) - V_{PV}(t_1) \tag{45}$$

$$dI_{PV}(t_2) \approx \Delta I_{PV}(t_2) = I_{PV}(t_2) - I_{PV}(t_1) \tag{46}$$

Therefore, analyzing Eq. (44), the first derivative can test whether the PV generator is operating at its MPP or far from it. Fig. 21 shows the flowchart implemented for the IC method.

$$\begin{cases} \frac{V_{PV}}{I_{PV}} = -\frac{\Delta V_{PV}}{\Delta I_{PV}} & \text{at MPP} \\ \frac{V_{PV}}{I_{PV}} < -\frac{\Delta V_{PV}}{\Delta I_{PV}} & \text{left to MPP} \\ \frac{V_{PV}}{I_{PV}} > -\frac{\Delta V_{PV}}{\Delta I_{PV}} & \text{right to MPP} \end{cases} \tag{47}$$

The main advantage of this algorithm is that it offers a good yield method under rapidly changing atmospheric conditions. Also, it achieves lower oscillations around the MPP than the P & O method, even though, when the P & O method is optimized, the MPPT efficiency of the IC and the P & O MPPT algorithms are essentially the same [68,83]. However, this method requires a complex control circuit.

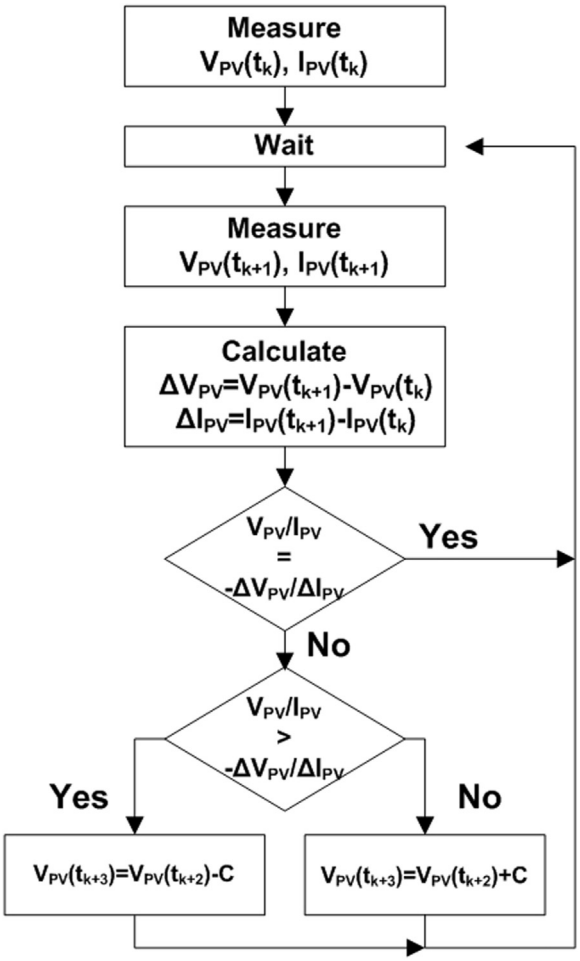

Fig. 21. Incremental conductance algorithm flowchart.

8.9. Method #31: Variable step incremental conductance method

The drawback of the IC method is the use of a fixed tracking step size. When this step is chosen large, the tracking speed becomes faster but contributes to excessive steady state oscillations in power. When chosen small, oscillations are reduced but the tracking process becomes slower. The modified IC method consists in varying the tracking step size [84], where the step value is automatically tuned depending on the distance between the operating point and the MPP. The step size increases when the MPP is far from the current point and decreases as it gets closer to the MPP. This method offers a fast tracking technique with a very low oscillation.

$$C = k\left|\frac{V_{PV}(n)I_{PV}(n) - V_{PV}(n-1)I_{PV}(n-1)}{V_{PV}(n) - V_{PV}(n-1)}\right| \tag{48}$$

where $V_{PV}(n)$ and $I_{PV}(n)$ are the output voltage and current of the PV module at the n^{th} sample of time. $V_{PV}(n-1)$ and $I_{PV}(n-1)$ are the output voltage and current of the PV module at the $(n-1)^{th}$ sample of time. k is a scaling factor for adjusting the step size.

8.10. Method #32: Variable step-size incremental-resistance method

This method is very similar to the previous one (Variable Step Incremental Conductance method), but the Incremental Resistance (INR) MPPT method is devoted to obtaining a simple and effective way to ameliorate both tracking dynamics and tracking accuracy [5,85]. The primary difference between this algorithm and the others is that the step-size modes of the INR MPPT can be switched by extreme values/points of a threshold function which is the product C of the exponential

of the PV array output power, P^n, and the absolute value of the PV array power derivative, $|dP/dI|$, as:

$$C = P^n \left| \frac{dP}{dI} \right| \tag{49}$$

where n is an index. The product of the first degree exponential (n=1) of the PV array power P and its derivative $|dP/dI|$ is applied to control the step size for the INR MPPT. Thus, the idea can be formulated as:

$$\begin{cases} \frac{\Delta C}{\Delta I} \geq 0 & \text{Fixed step-size mode (left of MPP)} \\ \frac{\Delta C}{\Delta I} < 0 & \text{Variable step-size mode (left of MPP)} \\ \frac{\Delta C}{\Delta I} > 0 & \text{Variable step-size mode (right of MPP)} \\ \frac{\Delta C}{\Delta I} \leq 0 & \text{Fixed step-size mode (right of MPP)} \end{cases} \tag{50}$$

where $\Delta C/\Delta I$ is the increment of the threshold function. Furthermore, the proposed variable step-size INR method is also based on the fact that the slope of the PV array power curve is zero at the MPP, positive on the left of the MPP, and negative on the right (see Fig. 4), thus the MPP can be tracked by comparing the instantaneous resistance (V/I) with the INR ($\Delta V/\Delta I$), as in Eq. (47).

8.11. Method #33: Parasitic capacitance (PC) method

This method is similar to the incremental conductance method, except that the effect of the PV cell parasitic junction capacitance, C_{ap}, is included [86]. Actually, there are two main reactive parasitic components called parasitic capacitance and parasitic inductance. The parasitic capacitance is developed by the accumulated charges in the junction area and the inductance is associated with the connections of the PV cells. It is reported that the *PC* reduces the error signal when the PV panel is operating outside the MPP, slowing down the system dynamics. However, these unavoidable losses are used as an important parameter in determining the MPP. By adding the capacitor current, I_C, to the PV current equation, a new equation is developed as:

$$I_{PV}(t) = I_{ph} - I_s(e^{\lambda(V_{PV}+I_{PV}R_s)} - 1) + C_{ap}\frac{dV_{PV}}{dt} \tag{51}$$

where I_C is expressed as:

$$I_C(t) = C_{ap}\frac{dV_{PV}}{dt} \tag{52}$$

Eq. (51) is reformulated as:

$$I_{PV}(t) = F(V_{PV}(t)) + C_{ap}\dot{V}_{PV}(t) \tag{53}$$

and the power is obtained as:

$$P_{PV}(t) == [F(V_{PV}(t)) + C_{ap}\dot{V}_{PV}(t)]V_{PV}(t) \tag{54}$$

Deriving the power in function of the panel voltage, then the condition of the MPP is fulfilled for:

$$\frac{dP_{PV}(t)}{dV_{PV}(t)} = \frac{dF(V_{PV}(t))}{dV_{PV}(t)}V_{PV}(t) + F(V_{PV}(t)) = 0 \tag{55}$$

therefore,

$$\frac{dF(V_{PV}(t))}{dV_{PV}(t)} = -\frac{F(V_{PV}(t))}{V_{PV}(t)} \tag{56}$$

where the left side of Eq. (56) represents the incremental conductance and the right side represents the instantaneous conductance. In this way, Eq. (56) can be rewritten as:

$$\dot{I}_{PV}(t)V_{PV}(t) = -I_{PV}(t)\dot{V}_{PV}(t) \tag{57}$$

The maximum power is transferred when doing the second derivative for the second term yields:

$$\frac{dF(V_{PV}(t))}{dV_{PV}(t)} + C\left(\frac{\ddot{V}_{PV}(t)}{\dot{V}_{PV}(t)} + \frac{\dot{V}_{PV}(t)}{V_{PV}(t)}\right) + \frac{F(V_{PV}(t))}{V_{PV}(t)} = 0 \tag{58}$$

where the dot represents the first derivative and the double-dot the second derivative. The three terms of Eq. (58) represent the incremental conductance, the induced ripple from the *PC* and the instantaneous conductance, respectively. The first and second derivatives take into account the AC ripple components generated by the converter. If the capacity value is assumed zero in Eq. (58), the equation of the *IC* algorithm is obtained. Parasitic capacity is modeled as a capacitor connected in parallel to each cell in a PV module. Therefore, the parallel connection of modules increases the amount of parasitic capacity, thus, the efficiency of the *PC* method is maximized in high-power PV systems that include numerous parallel-connected modules.

8.12. Method #34: β method

While a conventional method tracks the exact MPP, the β method tracks the maximum power using approximation. The analysis of the $I-V$ characteristics of a PV module leads to an intermediate variable,β, formulated as [31]:

$$\beta = \ln\left(\frac{I_{PV}}{V_{PV}}\right) - cV_{PV} = \ln(I_s c) \tag{59}$$

where I_s is the reverse saturation current and c is the diode constant given as $c = q/(AkTN_S)$ with q, A, k, T and Ns denoting the electronic charge, ideality factor, Boltzmann constant, temperature in Kelvin and the number of series connected cells, respectively. Thus, it can be seen from Eq. (59) that β depends only on temperature and not on irradiance.

It has been tested that for a given temperature the MPP magnitude variation is small compared with a wide variation of irradiance. Also, the magnitude variation is inversely proportional to the variation of temperature. Thus, it can be concluded that the magnitude of β at MPP lies within a small, fixed range (β_{min} to β_{max})when the temperature varies within a fixed range. The upper limit of β_{max} at MPP corresponds to the maximum irradiance and temperature. The lower limit of β_{min} at MPP corresponds to the minimum irradiance and temperature. While implementing the first stage of the algorithm, β_g, the value of β corresponding to the most probable module temperature is used as the guiding value for calculating the duty-cycle correction, M, while β_a denotes the actual value of β at a given instant.

It was observed from experimental tests that the value of β remains within a narrow band as the module operating point approaches the MPP. Therefore, by tracking β, the operating point can be quickly driven to the proximity of the MPP using large iterative steps. Subsequently, small steps (i.e. conventional MPPT techniques) can be employed to achieve the exact MPP. This method, based on β tracking,

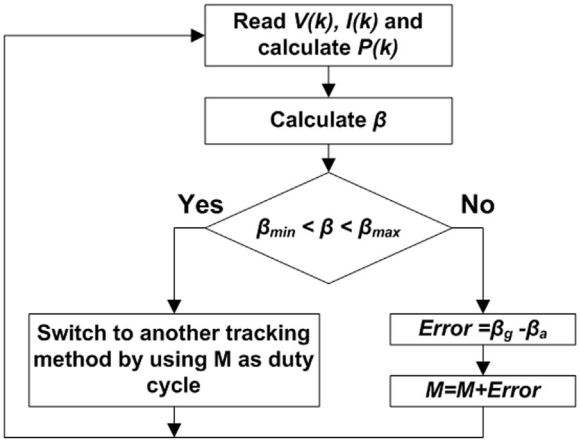

Fig. 22. The β method flowchart.

has the advantage of both fast and accurate tracking. The flowchart for the β method is shown in Fig. 22.

8.13. Method #35: I_{MPP} and V_{MPP} computation method

This method consists in computing I_{MPP} and V_{MPP} from the standard PV current equation involving the irradiance and the temperature levels. Once computed, a feedback control is used to force the PV module to operate at the MPP [87]. The PV voltage, V_{PV}, and current, I_{PV}, are described as follows:

$$I_{PV} = \left[I_S + I_{SC}\left(\frac{G}{G_{ref}} - 1\right) + \mu(T - T_{ref}) \right] N_P \tag{60}$$

$$V_{PV} = \left[V_S + \beta(T - T_{ref}) - R_s\left(\frac{1}{N_P} - I_S\right) - \frac{kI_{PV}}{N_P}(T - T_{ref}) \right] N_S \tag{61}$$

where V_S and I_S are the terminal voltage and the output current of a PV module, respectively. G and G_{ref} are the solar irradiance and the standard solar irradiance, respectively. T and T_{ref} are the temperature and the standard temperature, respectively. Moreover, I_{SC} is the short-circuit current at STC, μ is the temperature coefficient of I_{SC}, β is the temperature coefficient of the open-circuit voltage of the module, R_s is a series resistance of the module and k is the curve correction factor. N_S and N_P are the numbers of series and parallel connected modules.

The output power of the PV module is calculated by:

$$P_{PV} = V_{PV} I_{PV} = I_{PV}\left[V_S + \beta(T - T_{ref}) + R_s I_S - \frac{I_{PV}}{N_P}[R_s + k(T - T_{ref})] \right] N_S \tag{62}$$

Differentiating P_{PV} with respect to I_{PV} leads to the maximum voltage, V_{MPP}, and current, I_{MPP}.

$$I_{MPP} = \frac{N_P}{2} \frac{V_S + \beta(T - T_{ref}) + R_s I_S}{R_s + k(T - T_{ref})} \tag{63}$$

$$V_{MPP} = \frac{N_S}{2} V_S + \beta(T - T_{ref}) + R_s I_S \tag{64}$$

8.14. Method #36: Methods by modulation

This method consists in injecting a small ripple voltage to the PV voltage of operation. This leads to a power ripple whose phase and amplitude depends on the location of the local MPP [88]. When this modulation occurs on the left side of the MPP (zone "A") (see Fig. 23), the ripple voltage and the power will be perfectly in phase. However, when the modulation occurs on the right side of the MPP, (zone "B"), the ripples of the voltage and power will be out of phase. The amplitude of the power ripple signal shrinks as the operating point gets closer to the MPP. Therefore, the analysis of the phase and the amplitude provides clear information on the location of the MPP. However, this method suffers from the complexity and the difficulty of implementation as well the analysis of the low voltage output signal.

8.15. Method #37: Ripple correlation control

When a PV array is connected to a power converter, the switching action of the power converter imposes voltage and current ripple on the PV array. As a consequence, the PV array power is also subject to ripple [89]. Ripple Correlation Control (RCC) uses ripples to perform tracking. RCC correlates the time derivative of the time-varying PV array power with the time derivative of the time-varying PV array current or voltage to drive the power gradient to zero, thus reaching the MPP. If the voltage or the current increases and the power increases, then the operating point is below (to the left of) the MPP ($V < V_{MPP}$ or $I < I_{MPP}$). On the other hand, if the voltage or the current is increases and the power is decreases, then the operating point is above (to the right of) the MPP ($V > V_{MPP}$ or $I > I_{MPP}$).

9. Tracking techniques with intelligent prediction

9.1. Method #38: Fuzzy logic control

Trackers based on Fuzzy calculation are considered smart, since they track the MPP even if the inputs are imprecise. Fuzzy controllers do not need an accurate mathematical model. In general, fuzzy control consists of three stages, called fuzzification, rule base lookup table and defuzzification. In the first modeling stage, the numerical input variables are converted into linguistic variables based on a membership function, where five fuzzy levels are used: NB (negative big), NS

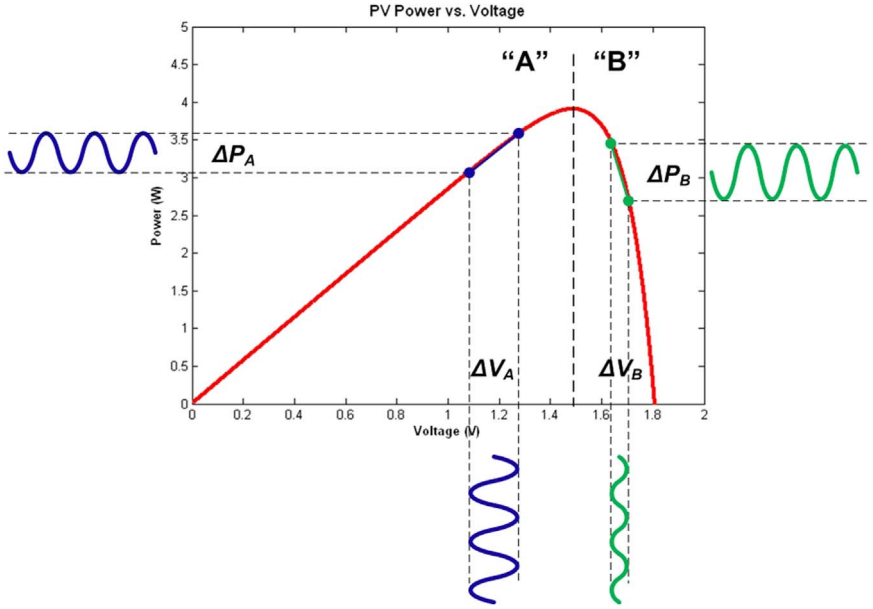

Fig. 23. Power ripples caused by voltage modulation. In zone "A", the voltage and phase ripples are in phase. In zone "B", power and voltage ripples are 180 degree out of phase.

(negative small), ZE (zero), PS (positive small) and PB (positive big). The inputs to an MPPT fuzzy logic controller are usually an error E and a change in error ΔE expressed as:

$$E(n) = \frac{V_{PV}(n)I_{PV}(n) - V_{PV}(n-1)I_{PV}(n-1)}{V_{PV}(n) - V_{PV}(n-1)} \quad (65)$$

and

$$\Delta E(n) = E(n) - E(n-1) \quad (66)$$

Once E and ΔE are calculated and converted to the linguistic variables, the output of the fuzzy controller, which is the change in duty-cycle ΔD of the power converter, can be found in the table shown in Fig. 24. In the defuzzification stage, the fuzzy logic controller output is converted from a linguistic variable to a numerical variable and provides an analog signal that will drive the power converter to the MPP. The MPPT fuzzy logic controller works well under varying atmospheric conditions. However, its effectiveness depends on choosing the right error computation and coming up with the rule base table [90,91].

9.2. Method #39: Neural network

The neural network technique is also considered a smart tracking techniques based on some environment learning process. It has three layers, called input, hidden and output layers, as shown in Fig. 25. The input variables can be the PV module parameters like V_{OC} and I_{SC}, the atmospheric data like irradiance and temperature, or any combination of these. The output represents the duty-cycle signal that drives the converter to track the MPP based on the algorithm used in the hidden layer. The link between nodes i and j is labeled as having a weight of ω_{ij} in Fig. 25. The neural network technique is based on weighting the links between nodes based on some training process, where the PV parameters are tested and recorded over months or years to get the right weight for every node. The drawback of this method is that the neural network has to be trained for the PV module in use and so cannot be generalized to work on several types at the same time unless trained to. Furthermore, the characteristics of the PV panel change with time, implying a periodical training of the neural network to accurately track the MPP [92].

9.3. Method #40: Biological swarm chasing algorithm

A smart technique was proposed in [93] for tracking the MPP in the same way as the Particle Swarm Optimization (PSO) technique. Swarm intelligence is an artificial intelligence technique involving the study of collective behavior in decentralized systems. One of the most popular swarm intelligence paradigms is the (PSO), which is basically developed through the simulation of the social behavior of bird flocking and fish schooling. In the proposed Bio-MPPT-based PV power system, each PV module is viewed as a particle, and the MPP is viewed as the moving target. Every PV module is designed to chase the MPP automatically by using the Bio-MPPT algorithm. Thus, by applying this method to a PV system, all modules in the PV array are assumed slaves for only one master module and each module has its own controller that communicates with the master controller to achieve the chasing of the MPP. Authors in [93] showed an efficiency enhancement of 12.19% compared to the P & O method.

10. Discussion

In this work, we have discussed forty methods on MPPT. Note that each technique has its own advantages and disadvantages concerning the tracking precision, the tracking speed, the component cost, and the implementation complexity. In addition, it is important to mention whatever the technique, the power plant size, by itself, imposes restrictions and compromises on the rules of the technique followed.

E \ ΔE	NB	NS	ZE	PS	PB
NB	ZE	ZE	NB	NB	NB
NS	ZE	ZE	NS	NS	NS
ZE	NS	ZE	ZE	ZE	PS
PS	PS	PS	PS	ZE	ZE
PB	PB	PB	PB	ZE	ZE

Fig. 24. Fuzzy rules table.

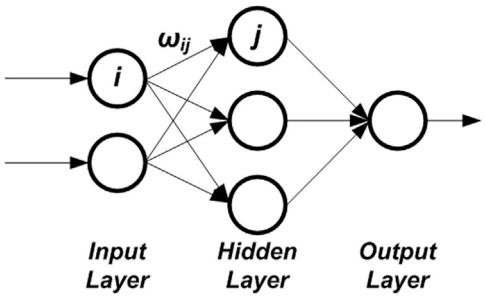

Fig. 25. Neural network layers.

For example, it is not efficient to implement a neural network tracker on a power plant of few hundred watts, even if it is more precise than the constant voltage method. Thus, one must take into account the tradeoff between the cost of the tracker and the revenue of the extra power extracted. The choice of the relevant strategy is depending on the considered use. In this study, we have presented each method by mentioning the limitations and the drawbacks of a complete tracking system, including speed, cost, precision, complexity, etc. To make it possible the choice of the more adequate approach, the MPPT techniques are classified based on their tracking methodology as presented in Table 2 that assesses the type of inputs, the type of sensors, the speed of tracking, the stability, and the tuning intervention. Nevertheless, we would like to stress, based on the literature reviews, that most papers deal with the P & O method, also, a market survey shows that the P & O based MPPTs are the most popular. This is not necessary an indicator of the perfectness of this algorithm, but it could be a suitable solution for manufacturers and for the end-user since this type of tracking technique can be implemented on all PV panels without knowing their characteristics. On the other hand, the IC method is also extensively used in literature and sometimes it is compared to the P & O method since it shows better performance toward the oscillation around the MPP. This is true from the point of view precision but concerning the implementation of the IC algorithm, the approach requires a controller with a floating-point core in order to solve differential equations, thus, higher cost compared to P & O circuit design. Generally speaking, the methods based artificial intelligence (see Table 2, lines 38–40) are the more faster and are very stable. However, the approaches are suitable only for digital applications and need at least two sensors. Besides, the methods with the possibility of period tuning (see Table 2, lines 1–6), even if they are fast, are unstable

Table 2
MPPT comparative table.

#	Tracking methods	A/D	Sensors	Speed	Stability	Periodic tuning
1	Constant Voltage	A	V	Fast	Not stable	Yes
2	Open-circuit voltage	A	V	Fast	Not stable	Yes
3	Short-circuit current	A	C	Fast	Not stable	Yes
4	Open-circuit voltage pilot PV cell method	A	V	Fast	Not stable	Yes
5	Temperature Gradient (TG) Algorithm	A	V	Fast	Not stable	Yes
6	Temperature Parametric (TP) Method	A	V	Fast	Not stable	Yes
7	Feedback voltage or current method	A	V or C	Slow	Not stable	No
8	P-N junction drop voltage tracking technique	A	V	Fast	Not stable	Yes
9	Look-up table	D	I & T	Fast	Depends on memory	Yes
10	Load current or load voltage maximization	A	V or C	Slow	Not stable	No
11	Linear Current Control	D	V & C	Slow	Stable	No
12	The only current photovoltaic	A	C	Slow	Not stable	No
13	PV Output Senseless (POS) Control	D	C	Slow	Not stable	No
14	Perturb and observe	A/D	V & C	Slow	Not stable	No
15	Modified P & O With Fixed Perturb	D	V & C	Slow	Stable	No
16	Conv P & O With Adaptive Perturb	D	V & C	Fast	Not stable	No
17	Modified P & O With Adaptive Perturb	D	V & C	Fast	Stable	No
18	Three-Point Weight Comparison	D	V & C	Fast	Stable	No
19	On-Line MPP Search Algorithm	D	V & C	Slow	Stable	No
20	DC-Link Capacitor Droop Control	D	V & C	Slow	Stable	No
23	State-based MPPT Method	D	V & C	Slow	Stable	No
24	Linear Reoriented Coordinates	D	V & C	Slow	Stable	No
25	Curve-fitting	D	V	Fast	Not stable	Yes
26	Differentiation method	D	V & C	Slow	Stable	No
27	Slide Control Method	D	V & C	Very fast	Stable	No
28	Current Sweep	D	V & C	Slow	Stable	No
29	dP/dV or dP/dI Feedback Control	D	V & C	Slow	Stable	No
30	Incremental Conductance	D	V & C	Slow	Stable	No
31	Variable Step IC	D	V & C	Fast	Stable	No
32	Variable Step-Size Incremental-Resistance	D	V & C	fast	Stable	No
33	Parasitic capacitance	D	V & C	Fast	Stable	No
34	β method	D	V & C	Slow	Stable	No
35	I_{MPP} and V_{MPP} Computation	D	I & T	Fast	Not stable	No
36	Methods by modulation	D	V & C	Slow	Very stable	No
37	Ripple Correlation Control	D	V & C	Slow	Very stable	No
38	Fuzzy Logic Control	D	V & C	Very fast	Very stable	No
39	Neural Network	D	V & C	Very fast	Very stable	No
40	Biological Swarm Chasing Algorithm	D	V & C	Very fast	Very stable	No

and available only for applications with alternative current. Finally, and based on the pre-mentioned reasons, the selection of the adequate method is depending on the use and its design criteria (accuracy, cost, etc).

11. Conclusion

From about 20 years, researchers and scientists are working to increase the efficiency of renewable energy systems and the MPPT is one of the fields that attracted the interest of many researcher since it focuses on finding new algorithm to extract as much power from the source. In this paper, 40 methods for MPPT, applied mainly on PV systems, are cited where the entire methods focus on how to extract the maximum power regardless the complexity of calculation and implementation. It is focused on the algorithm of tracking and the advantages and disadvantages of each method taking into consideration the implementation complexity.

References

[1] Karami N, Outbib R, Moubayed N. Fuel flow control of a pem fuel cell with mppt. In: Proceedings of the IEEE international symposium on intelligent control (ISIC), IEEE; 2012. p. 289–94.

[2] Karami N, Moubayed N, Outbib R. Maximum power point tracking with reactant flow optimization of proton exchange membrane fuel cell. J Fuel Cell Sci Technol 2013;10(5):14.

[3] Karami N, Moubayed N. New modeling approach and validation of a thermoelectric generator. In: Proceedings of the IEEE ISIE international symposium on industrial electronics, IEEE; 2014. p. 586–91.

[4] Dunlop J. Batteries and charge control in stand-alone photovoltaic systems fundamentals and application. Sandia National Laboratories.

[5] Ali A, Saied M, Mostafa M, Abdel-Moneim T. A survey of maximum ppt techniques of pv systems. In: Energytech, IEEE; 2012. p. 1–17.

[6] ElAyoubi A, Nazih M. Renewable sources grid connected converters. In: Proceedings of the 6th international conference on electrical and power engineering; 28–30 Octobre 2010. p. 172–7.

[7] Nazih M, Ali E, Rachid O. Control of an hybrid solar-wind system with acid battery for storage. In: Proceedings of the WSEAS transactions on power systems, vol. 4(9); Sep. 2009. p. 307–18.

[8] Chunhua L, Chau K, Xiaodong Z. An efficient wind -photovoltaic hybrid generation system using doubly excited permanent-magnet brushless machine. IEEE Trans Ind Electron 2010;57(3):831–9.

[9] Esram T, Chapman P. Comparison of photovoltaic array maximum power point tracking techniques. IEEE Trans Energy Convers 2007;22(2):439–49. http://dx.doi.org/10.1109/TEC.2006.874230.

[10] Overall Efficiency of Grid Connected Photovoltaic Inverters. Tech. rep., European Standard EN 50530; 2010.

[11] Wehbe J, Karami N. Battery equivalent circuits and brief summary of components value determination of lithium ion: A review. In: Proceedings of the third international conference on technological advances in electrical, electronics and computer engineering (TAEECE), vol. 201(5); 2015. p. 45–9.⟨http://dx.doi.org/10.1109/TAEECE.2015.7113598⟩.

[12] Tarabay J, Karami N. Nickel metal hydride battery: Structure, chemical reaction, and circuit model. In: Proceedings of the third international conference on technological advances in electrical, electronics and computer engineering (TAEECE); 2015; p. 22–26. ⟨http://dx.doi.org/10.1109/TAEECE.2015.7113594⟩.

[13] El Ghossein N, Salameh J, Karami N, El Hassan M, Najjar M. Survey on electrical modeling methods applied on different battery types. In: Proceedings of the third internationalconference on technological advances in electrical, electronics and computer engineering (TAEECE); 2015. p. 39–44. ⟨http://dx.doi.org/10.1109/TAEECE.2015.7113597⟩.

[14] Karami N, Moubayed N, Outbib R. Analysis and implementation of an adaptative pv based battery floating charger. Sol Energy 2012;86(9):2383–96. http://dx.doi.org/10.1016/j.solener.2012.05.009.

[15] Fattal J, Bou Dib P, Karami N. Review on different charging techniques of a lithium polymer battery. In: Proceedings of the third international conference on technological advances in electrical, electronics and computer engineering (TAEECE); 2015. p. 33–8. ⟨http://dx.doi.org/10.1109/TAEECE.2015.7113596⟩.

[16] Horkos P, Yammine E, Karami N. in: Review on different charging techniques of

lead-acid batteries. In: Proceedings of the third international conference on technological advances in electrical, electronics and computer engineering (TAEECE); 2015. p. 27–32. ⟨http://dx.doi.org/10.1109/TAEECE.2015.7113595⟩.
[17] Ayoub E, Karami N. Review on the charging techniques of a li-ion battery. In: Proceedings of the third international conference on technological advances in electrical, electronics and computer engineering (TAEECE); 2015. p. 50–55. ⟨http://dx.doi.org/10.1109/TAEECE.2015.7113599⟩.
[18] Yu G, Jung Y, Choi J, Choy I, Song J, Kim G. A novel two-mode mppt control algorithm based on comparative study of existing algorithms. In: Proceedings of the conference record of the twenty-ninth IEEE photovoltaic specialists conference; 2002, p. 1531–34. ⟨http://dx.doi.org/10.1109/PVSC.2002.1190903⟩.
[19] Wasynczuk O. Dynamic behavior of a class of photovoltaic power systems. IEEE PER Power Eng Rev 1983;3(9):36–7. http://dx.doi.org/10.1109/MPER.1983.5519293.
[20] Shimizu T, Hashimoto O, Kimura G. A novel high-performance utility-interactive photovoltaic inverter system. IEEE Trans Power Electron 2003;18(2):704–11. http://dx.doi.org/10.1109/TPEL.2003.809375.
[21] Koutroulis E, Kalaitzakis K, Voulgaris N. Development of a microcontroller-based, photovoltaic maximum power point tracking control system. IEEE Trans Power Electron 2001;16(1):46–54. http://dx.doi.org/10.1109/63.903988.
[22] Veerachary M, Senjyu T, Uezato K. Maximum power point tracking control of idb converter supplied pv system. IEE Proc Electr Power Appl 2001;148(6):494–502. http://dx.doi.org/10.1049/ip-epa:20010656.
[23] Xiao W, Dunford W. A modified adaptive hill climbing mppt method for photovoltaic power systems. In: Proceedings of the power electronics specialists conference, vol. 3; 2004. p. 1957–63. ⟨http://dx.doi.org/10.1109/PESC.2004.1355417⟩.
[24] Al-Amoudi A, Zhang L. Optimal control of a grid-connected pv system for maximum power point tracking and unity power factor. In: Proceedings of the seventh international conference on power electronics and variable speed drives; 1998. p. 80–5. ⟨http://dx.doi.org/10.1049/cp:19980504⟩.
[25] Kasa N, Lida T, Iwamoto H. Maximum power point tracking with capacitor identifier for photovoltaic power system. IEE Proc Electr Power Appl 2000;147(6):497–502. http://dx.doi.org/10.1049/ip-epa:20000641.
[26] Zhang L, Amoudi A, Bai Y. Real-time maximum power point tracking for grid-connected photovoltaic systems. In: Proceedings of the power electronics and variable speed drives; 2000, p. 124–9. ⟨http://dx.doi.org/10.1049/cp:20000232⟩.
[27] Hua C-C, Lin J-R. Fully digital control of distributed photovoltaic power systems. In: Proceedings of the IEEE international symposium on industrial electronics, vol. 1; 2001. p. 1–6. ⟨http://dx.doi.org/10.1109/ISIE.2001.931745⟩.
[28] Chiang M-L, Hua C-C, Lin J-R. Direct power control for distributed pv power system. In: Proceedings of the power conversion conference, vol. 1; 2002. p. 311–5. ⟨http://dx.doi.org/10.1109/PCC.2002.998566⟩.
[29] Chomsuwan K, Prisuwanna P, Monyakul V. Photovoltaic grid-connected inverter using two-switch buck-boost converter. In: Proceedings of the photovoltaic specialists conference; 2002, p. 1527–30. ⟨http://dx.doi.org/10.1109/PVSC.2002.1190902⟩.
[30] Park M, Yu I-K. A study on the optimal voltage for mppt obtained by surface temperature of solar cell. In: Proceedings of the 30th annual conference of IEEE industrial electronics society, IECON, vol. 3; 2004. p. 2040–45.
[31] Jain S, Agarwal V. A new algorithm for rapid tracking of approximate maximum power point in photovoltaic systems. IEEE Power Electron Lett 2004;2(1):16–9. http://dx.doi.org/10.1109/LPEL.2004.828444.
[32] Tafticht T, Agbossou K. Development of a mppt method for photovoltaic systems. In: Proceedings of the Canadian conference on electrical and computer engineering, vol. 2; 2004. p. 1123–26. ⟨http://dx.doi.org/10.1109/CCECE.2004.1345317⟩.
[33] Kobayashi K, Matsuo H, Sekine Y. An excellent operating point tracker of the solar-cell power supply system. IEEE Trans Ind Electron 2006;53(2):495–9. http://dx.doi.org/10.1109/TIE.2006.870669.
[34] Kim Y, Jo H, Kim D. A new peak power tracker for cost-effective photovoltaic power system. In: Proceedings of the energy conversion engineering conference, vol. 3; 1996. p. 1673–78. ⟨http://dx.doi.org/10.1109/IECEC.1996.553353⟩.
[35] Kislovski A, Redl R. Maximum-power-tracking using positive feedback. In: Proceedings of the power electronics specialists conference, 25th Annual IEEE, vol. 2; 1994. p. 1065–68. ⟨http://dx.doi.org/10.1109/PESC.1994.373812⟩.
[36] Valderrama-Blavi H, Alonso C, Martinez-Salamero L, Singer S, Estibals B, Maixe-Altes J. Ac-lfr concept applied to modular photovoltaic power conversion chains. IEE Proc Electr Power Appl 2002;149(6):441–8. http://dx.doi.org/10.1049/ip-epa:20020479.
[37] Arias J, Linera F, Martin-Ramos J, Pernia A, Cambronero J. A modular pv regulator based on microcontroller with maximum power point tracking. In: Proceedings of the industry applications conference, vol. 2; 2004. p. 1178–84. ⟨http://dx.doi.org/10.1109/IAS.2004.1348562⟩.
[38] Shmilovitz D. On the control of photovoltaic maximum power point tracker via output parameters. IEE Proc Electr Power Appl 2005;152(2):239–48. http://dx.doi.org/10.1049/ip-epa:20040978.
[39] Salas V, Olias E, Lazaro A, Barrado A. New algorithm using only one variable measurement applied to a maximum power point tracker. Sol Energy Mater Sol Cells 2005;87(1–4):675–84. http://dx.doi.org/10.1016/j.solmat.2004.09.019.
[40] Pan C-T, Chen J-Y, Chu C-P, Huang Y-S. A fast maximum power point tracker for photovoltaic power systems. In: Proceedings of the industrial electronics society, vol. 1; 1999. p. 390–93. ⟨http://dx.doi.org/10.1109/IECON.1999.822229⟩.
[41] Salas V, Olias E, Lazaro A, Barrado A. Evaluation of a new maximum power point tracker (mppt) applied to the photovoltaic stand-alone systems. Solar Energy Materials and Solar Cells.
[42] Patel H, Agarwal V. Mppt scheme for a pv-fed single-phase single-stage grid-connected inverter operating in ccm with only one current sensor. IEEE Trans Energy Convers 2009;24(1):256–63.
[43] Lee S-J, Park H-Y, Kim G-H, Seo H-R, Ali M, Park M, et al. The experimental analysis of the grid- connected pv system applied by pos mppt. In: Proceedings of the international conference on electrical machines and systems, ICEMS; 2007. p. 1786–91.
[44] Femia N, Petrone G, Spagnuolo G, Vitelli M. Optimization of perturb and observe maximum power point tracking method. IEEE Trans Power Electron 2005;20(4):963–73. http://dx.doi.org/10.1109/TPEL.2005.850975.
[45] Wolfs P, Tang L. A single cell maximum power point tracking converter without a current sensor for high performance vehicle solar arrays. In: Proceedings of the power electronics specialists conference; 2005. p. 165–71. ⟨http://dx.doi.org/10.1109/PESC.2005.1581619⟩.
[46] D'Souza N, Lopes L, Liu X. An intelligent maximum power point tracker using peak current control. In: Proceedings of the power electronics specialists conference; 2005. p. 172. ⟨http://dx.doi.org/10.1109/PESC.2005.1581620⟩.
[47] Pandey A, Dasgupta N, Mukerjee A. High-performance algorithms for drift avoidance and fast tracking in solar mppt system. IEEE Trans Energy Convers 2008;23(2):681–9. http://dx.doi.org/10.1109/TEC.2007.914201.
[48] Sefa I, Ozdemir O. Experimental study of interleaved mppt converter for pv systems. In: Proceedings of the industrial electronics, IECON, 35th annual conference of IEEE; 2009. p. 456–61. ⟨http://dx.doi.org/10.1109/IECON.2009.5414965⟩.
[49] Jain S, Agarwal V. Comparison of the performance of maximum power point tracking schemes applied to single-stage grid-connected photovoltaic systems. IET Electr Power Appl 2007;1(5):753–62. http://dx.doi.org/10.1049/iet-epa:20060475.
[50] Desai H, Patel H. Maximum power point algorithm in pv generation: an overview. In: Proceedings of the international conference on power electronics and drive systems; 2007. p. 624–30. ⟨http://dx.doi.org/10.1109/PEDS.2007.4487766⟩.
[51] Wasynczuk O. Dynamic behavior of a class of photovoltaic power systems. IEEE PER Power Eng Rev 1983;3(9):36–7. http://dx.doi.org/10.1109/MPER.1983.5519293.
[52] Hua C, Lin JR. Dsp-based controller application in battery storage of photovoltaic system. In: Proceedings of the 1996 IEEE IECON 22nd international conference on industrial electronics, control, and instrumentation, vol. 3; 1996. p. 1705–10. ⟨http://dx.doi.org/10.1109/IECON.1996.570673⟩.
[53] Jung Y, Yu G, Choi J, Choi J. High-frequency dc link inverter for grid-connected photovoltaic system. In: Proceedings of the photovoltaic specialists conference; 2002. p. 1410–3. ⟨http://dx.doi.org/10.1109/PVSC.2002.1190873⟩.
[54] Femia N, Lisi G, Petrone G, Spagnuolo G, Vitelli M. Distributed maximum power point tracking of photovoltaic arrays: novel approach and system analysis. IEEE Trans Ind Electron 2008;55(7):2610–21. http://dx.doi.org/10.1109/TIE.2008.924035.
[55] Fortunato M, Giustiniani A, Petrone G, Spagnuolo G, Vitelli M. Maximum power point tracking in a one-cycle-controlled single-stage photovoltaic inverter. IEEE Trans Ind Electron 2008;55(7):2684–93. http://dx.doi.org/10.1109/TIE.2008.918463.
[56] Figueres E, Garcera G, Sandia J, Gonzalez-Espin F, Rubio J. Sensitivity study of the dynamics of three-phase photovoltaic inverters with an lcl grid filter. IEEE Trans Ind Electron 2009;56(3):706–17. http://dx.doi.org/10.1109/TIE.2008.2010175.
[57] Patel H, Agarwal V. Investigations into the performance of photovoltaics-based active filter configurations and their control schemes under uniform and non-uniform radiation conditions. IET Renew Power Gener 2010;4(1):12–22. http://dx.doi.org/10.1049/iet-rpg.2008.0081.
[58] Park S-H, Cha G-R, Jung Y-C, Won C-Y. Design and application for pv generation system using a soft-switching boost converter with sarc. IEEE Trans Ind Electron 2010;57(2):515–22. http://dx.doi.org/10.1109/TIE.2009.2036025.
[59] Slonim M, Rahovich L. Maximum power point regulator for 4 kw solar cell array connected through invertor to the ac grid. In: Proceedings of the energy conversion engineering conference, vol. 3; 1996. p. 1669–72. ⟨http://dx.doi.org/10.1109/IECEC.1996.553352⟩.
[60] Hsiao Y-T, Chen C-H. Maximum power tracking for photovoltaic power system. In: Proceedings of the industry applications conference, vol. 2; 2002. p. 1035–40. ⟨http://dx.doi.org/10.1109/IAS.2002.1042685⟩.
[61] Kasa N, Iida T, Chen L. Flyback inverter controlled by sensorless current mppt for photovoltaic power system. IEEE Trans Ind Electron 2005;52(4):1145–52. http://dx.doi.org/10.1109/TIE.2005.851602.
[62] Jain S, Agarwal V. A single-stage grid connected inverter topology for solar pv systems with maximum power point tracking. IEEE Trans Power Electron 2007;22(5):1928–40. http://dx.doi.org/10.1109/TPEL.2007.904202.
[63] Gules R, De Pellegrin Pacheco J, Hey H, Imhoff J. A maximum power point tracking system with parallel connection for pv stand-alone applications. IEEE Trans Ind Electron 2008;55(7):2674–83. http://dx.doi.org/10.1109/TIE.2008.924033.
[64] Jung K, Bong K, Kwang N. Three-phase photovoltaic system with three-level boosting mppt control. IEEE Trans Power Electron 2008;23(5):2319–27.
[65] Bong K, Kwang N, Jung K. Grid-connected photovoltaic multistring pcs with pv current variation reduction control. IEEE Trans Ind Electron 2009;56(11):4381–8.
[66] Piegari L, Rizzo R. Adaptive perturb and observe algorithm for photovoltaic maximum power point tracking. IET Renew Power Gener 2010;4(4):317–28. http://dx.doi.org/10.1049/iet-rpg.2009.0006.
[67] Femia N, Petrone G, Spagnuolo G, Vitelli M. Optimizing duty-cycle perturbation of p and o mppt technique. In: Proceedings of the power electronics specialists conference, vol. 3; 2004. p. 1939–44.
[68] Liu X, Lopes L. An improved perturbation and observation maximum power point

tracking algorithm for pv arrays. In: Proceedings of the power electronics specialists conference, vol. 3; 2004. p. 2005–10.
[69] Altas I, Sharaf A. A novel on-line mpp search algorithm for pv arrays. IEEE Trans Energy Convers 1996;11(4):748–54.
[70] Matsui M, Kitano T, hong Xu D, qing Yang Z. A new maximum photovoltaic power tracking control scheme based on power equilibrium at dc link. In: Proceedings of the industry applications conference, vol. 2; 1999. p. 804–9. ⟨http://dx.doi.org/10.1109/IAS.1999.801599⟩.
[71] Kitano T, Matsui M, Hong Xu D. Power sensor-less mppt control scheme utilizing power balance at dc link-system design to ensure stability and response. In: Proceedings of the industrial electronics society, vol. 2; 2001. p. 1309–14. ⟨http://dx.doi.org/10.1109/IECON.2001.975971⟩.
[72] El-Shibini M, Rakha H. Maximum power point tracking technique. In: Electrotechnical conference, 1989. Proceedings integrating research, industry and education in energy and communication engineering, MELECON '89, Mediterranean; 1989. p. 21–4.
[73] Zhang L, W H, W W. A new approach to achieve maximum power point tracking for pv system with a variable inductor. IEEE Trans Power Electron 2011;26(4):1031–7.
[74] Solodovnik E, Liu S, Dougal R. Power controller design for maximum power tracking in solar installations. IEEE Trans Power Electron 2004;19(5):1295–304.
[75] rtiz Rivera E, Peng F. A novel method to estimate the maximum power for a photovoltaic inverter system. in: Proceedings of the 35th IEEE annual power electronics specialists conference, PESC, vol. 3; 2004. p. 2065–69.
[76] Faranda R, Leva S, Maugeri V. Mppt techniques for pv systems: energetic and cost comparison. In: Proceedings of the power and energy society; 2008. p. 1–6. ⟨http://dx.doi.org/10.1109/PES.2008.4596156⟩.
[77] Lopez-Seguel J, Seleme S, Donoso-Garcia P, Morais L, Cortizo P, Mendes M. Comparison of mppt approaches in autonomous photovoltaic energy supply system using dsp. In: Proceedings of the international conference on industrial technology (ICIT); 2010., p. 1149–54. ⟨http://dx.doi.org/10.1109/ICIT.2010.5472594⟩.
[78] Teulings W, Marpinard J, Capel A, O'Sullivan D. A new maximum power point tracking system, In: Proceedings of the power electronics specialists conference, 24th Annual IEEE; 1993. p. 833–8. ⟨http://dx.doi.org/10.1109/PESC.1993.472018⟩.
[79] Zhang M, Wu J, Zhao H. The application of slide technology in pv maximum power point tracking system. In: Proceedings of the fifth world congress on intelligent control and automation, vol. 6; 2004. p. 5591–94
[80] Bodur M, Ermis M. Maximum power point tracking for low power photovoltaic solar panels. In: Proceedings of the 7th mediterranean electrotechnical conference, vol. 2; 1994. p. 758–61.
[81] Sugimoto H, Dong H. A new scheme for maximum photovoltaic power tracking control. In: Proceedings of the power conversion conference, vol. 2; 1997. p. 691–96.
[82] Hussein K, Muta I, Hoshino T, Osakada M. Maximum photovoltaic power tracking: an algorithm for rapidly changing atmospheric conditions. IEE Proc Gener Transm Distrib 1995;142(1):59–64. http://dx.doi.org/10.1049/ip-gtd:19951577.
[83] Hohm D, Ropp M. Comparative study of maximum power point tracking algorithms using an experimental, programmable, maximum power point tracking test bed. In: Proceedings of the conference record of the twenty-proceedings of the eighth IEEE photovoltaic specialists conference; 2000. p. 1699–702.
[84] Liu F, Duan S, Liu F, Liu B, Kang Y. A variable step size inc mppt method for pv systems. IEEE Trans Ind Electron 2008;55(7):2622–8.
[85] Mei Q, Shan M, Liu L, Guerrero J. A novel improved variable step-size incremental-resistance mppt method for pv systems. IEEE Trans Ind Electron 2011;58(6):2427–34.
[86] Brambilla A, Gambarara M, Garutti A, Ronchi F. New approach to photovoltaic arrays maximum power point tracking. In: Proceedings of the power electronics specialists conference, vol. 2; 1999. p. 632–37.
[87] Takashima T, Tanaka T, Amano M, Ando Y. Maximum output control of photovoltaic (pv) array. In: Proceedings of the energy conversion engineering conference and exhibit, vol. 1; 2000. p. 380–3.
[88] Tse K, Chung H, Hui S, Ho M. A novel maximum power point tracking technique for pv panels. In: Proceedings of the power electronics specialists conference, PESC. 2001 IEEE 32nd Annual, vol. 4; 2001. p. 1970–5.
[89] Midya P, Krein P, Turnbull R, Reppa R, Kimball J. Dynamic maximum power point tracker for photovoltaic applications. In: Proceedings of the power electronics specialists conference, 1996. PESC '96 Record., 27th Annual IEEE, vol. 2; 1996. p. 1710–16.
[90] Hilloowala R, Sharaf A. A rule-based fuzzy logic controller for a pwm inverter in photo-voltaic energy conversion scheme. In: Proceedings of the industry applications society, vol.1; 1992. p. 762–69.
[91] Kottas T, Boutalis Y, Karlis A. New maximum power point tracker for pv arrays using fuzzy controller in close cooperation with fuzzy cognitive networks. IEEE Trans Energy Convers 2006;21(3):793–803.
[92] Hiyama T, Kouzuma S, Imakubo T. Identification of optimal operating point of pv modules using neural network for real time maximum power tracking control. IEEE Trans Energy Convers 1995;10(2):360–7.
[93] Chen L-R, Tsai C-H, Lin Y-L, Lai Y-S. A biological swarm chasing algorithm for tracking the pv maximum power point. IEEE Trans Energy Convers 2010;25(2):484–93.